Published in final edited form as:
Glia. 2010 October ; 58(13): 1553–1569. doi:10.1002/glia.21029.

Origin, Maturation and Astroglial Transformation of Secondary Radial Glial Cells in the Developing Dentate Gyrus

Bianka Brunne[1,2], **Shanting Zhao**[2], **Amin Derouiche**[3], **Joachim Herz**[1,4], **Petra May**[1,5], **Michael Frotscher**[1,2], and **Hans H. Bock**[1,5,*]

[1]Center of Neurosciences, University of Freiburg, Albertstrasse 23, D-79104 Freiburg, Germany

[2]Institute of Anatomy and Cell Biology, University of Freiburg, Albertstrasse 17, D-79104 Freiburg, Germany

[3]Institute of Cellular Neurosciences, University of Bonn, Sigmund-Freud-Str. 25, D-53105 Bonn, Germany

[4]Department of Molecular Genetics, University of Texas Southwestern Medical Center, 5323 Harry Hines Blvd., Dallas, TX 75390-9046, U.S.A.

[5]Department of Medicine II, University Hospital Freiburg, Hugstetter Strasse 55, D-79106 Freiburg, Germany.

Abstract

The dentate gyrus is a brain region where neurons are continuously born throughout life. In the adult, the role of its radial glia in neurogenesis has attracted much attention over the past years, however, little is known about the generation and differentiation of glial cells and their relationship to radial glia during the ontogenetic development of this brain structure. Here, we combine immunohistochemical phenotyping using antibodies against glial marker proteins with BrdU birthdating to characterize the development of the secondary radial glial scaffold in the dentate gyrus and its potential to differentiate into astrocytes. We demonstrate that the expression of BLBP, GLAST and GFAP characterizes immature differentiating cells confined to an astrocytic fate in the early postnatal dentate gyrus. Based on our studies we propose a model where immature astrocytes migrate radially through the granule cell layer to adopt their final positions in the molecular layer of the dentate gyrus. Time-lapse imaging of acute hippocampal slices from hGFAP-eGFP transgenic mice provide direct evidence for such a migration mode of differentiating astroglial cells in the developing dentate gyrus.

Keywords

gliogenesis; hippocampus; time-lapse microscopy; fatty acid-binding protein 7 (Fabp7); development

Introduction

The dentate gyrus is one of the few brain areas where progenitor cells proliferate and generate neurons throughout life in an activity-regulated manner (Gage et al. 1998; Ming and Song 2005). Understanding the mechanisms governing its morphological development is therefore

*Corresponding author: Hans H. Bock Zentrum für Neurowissenschaften, University of Freiburg Albertstrasse 23, D-79104 Freiburg Tel. +49-(0)761-203 8421, Fax +49-(0)761-203 8417 Hans.Bock@zfn.uni-freiburg.de.

essential for a full comprehension of the functions of the dentate gyrus, including its capacity to generate new neurons during adulthood. Dentate histogenesis is characterized by the successive establishment of different proliferative zones, resulting in a prolonged period of granule cell neurogenesis (Altman and Bayer 1990a; Altman and Bayer 1990b; Cowan et al. 1980; Frotscher and Seress 2007; Reznikov 1991). The first granule cells originate from the ventricular germinal zone near the prospective fimbria and migrate into the incipient dentate area along a primordial radial glial scaffold that extends from the fimbria to the pial surface (Eckenhoff and Rakic 1984; Li et al. 2009; Rickmann et al. 1987). Around birth, the main proliferative zone shifts into the dentate area, including - but not limited to - the hilar region, while the primordial radial glial scaffold disappears. Within the first week after birth, a secondary radial glial scaffold develops (Bignami and Dahl 1974; Rickmann et al. 1987; Sievers et al. 1992). Its cell bodies are located in the subgranular zone and extend their prominent radial processes through the granular into the molecular layer. From the second postnatal week, progenitor proliferation is limited to the subgranular zone, where neurogenesis continues into adulthood.

Radial glial cells, originally viewed as mere migration support of radially locomoting neurons, constitute a heterogeneous population of regionally different precursor cells that can give rise to both neurons and glial cells (Kriegstein and Gotz 2003; Pinto and Gotz 2007; Rakic 2003). In the adult dentate gyrus it has been demonstrated that subgranular radial glial-like cells function as neural and glial precursors (Garcia et al. 2004; Kempermann et al. 2004; Seri et al. 2004; Seri et al. 2001). Surprisingly, the function of the secondary radial glial cells during organogenesis of the dentate gyrus is less well understood. Since the secondary radial glial scaffold is fully developed as late as in the second postnatal week, it does not only contribute to the generation of granule neurons, which are mainly formed pre- and perinatally (Altman and Bayer 1990a; Cowan et al. 1980; Namba et al. 2005; Reznikov 1991). Furthermore, the granule cell layer develops in a radial outside-in-gradient (Eckenhoff and Rakic 1984; Martin et al. 2002; Stanfield and Cowan 1979) with the apposition of young neurons close to their site of origin, not necessarily requiring a glia-guided migration step as in the neocortex or hippocampus proper (Nadarajah and Parnavelas 2002). These findings argue against a prominent role of the secondary radial glia as a migratory scaffold for immature granule neurons along its processes. It has been suggested that the long unbranched processes of radial glia might convey signals to the nucleus that reflect the state of the local environment, thereby instructing differentiating cells to adopt region- and context-specific phenotypes (Hall et al. 2003). Other putative functions of the secondary radial glia might include the promotion of dendritic outgrowth of newborn neurons (Shapiro et al. 2005), the arrangement of dentate granule cells into a compact layer (Zhao et al. 2004), and their transformation into astrocytes (Eckenhoff and Rakic 1984).

In this study, we present an immunohistochemical marker profile of dentate gyrus development that reflects the spatiotemporal development and maturation of the secondary radial glial scaffold with special emphasis on its role in astroglial differentiation. By combining immunohistochemistry and BrdU birthdating studies we provide direct evidence that secondary radial glial cells originate from the secondary precursor cell pool in the dentate gyrus. Based on our marker profile we demonstrate that glial fibrillary acidic protein (GFAP) and brain lipid binding protein (BLBP), a molecular marker of radial glia in different brain regions (Anthony and Heintz 2008; Feng et al. 1994; Hartfuss et al. 2001; Kurtz et al. 1994), label immature astroglial cells in the early postnatal dentate gyrus. Using these markers we demonstrate the translocation of transforming secondary radial glia not only on a morphological but also on an immunohistochemical level, and provide evidence that these terminally differentiating cells migrate outwards through the granule cell layer to adopt their final position and astrocytic fate in the molecular layer of the dentate gyrus. This migration mode of astroglial-committed cells

was directly visualized by time-lapse microscopy of postnatal organotypic hippocampal slice cultures from hGFAP-eGFP transgenic mice.

Materials and Methods

Tissue Preparation for Immunohistochemistry

For timed matings, the day of vaginal plug detection was counted as embryonic day 0.5 (E0.5). The day of birth was counted as postnatal day 0 (P0). Brains for immunohistochemistry were obtained from 16 young in-house-bred NMRI mice (P0, P3, P10, P21; four animals/age), four adult NMRI mice (3-5 months), 28 young in-house-bred wildtype mice on a C57BL/6JxSv129Ev background (E16.5, P0, P3, P6, P10, P14, P21; four animals/age), 9 young in-house-bred Wistar rats (P3, P10, P21; three animals/age) and 2 young (P7) heterozygous hGFAP-eGFP mice (Nolte et al. 2001). No differences between wildtype strains were noted. All animals were maintained in accordance with the institutional guidelines for animal care at the University of Freiburg (license no. 35-9185.81/3/437).

Animals older than P6 were killed with CO_2 and perfused intracardially with phosphate-buffered saline (PBS) followed by 4% paraformaldehyde (PFA) in PBS. Brains were postfixed in 4% PFA at 4°C overnight. The brains of younger animals were dissected after decapitation under hypothermic anaesthesia and immersion-fixed in 4% PFA in PBS at 4°C overnight.

Immunohistochemistry and Microscopy

Brains were embedded in 5% agar and cut into 50 μm coronal sections using a Leica-VT1000S vibratome (Leica, Nussloch, Germany). To include sections from different septo-temporal areas of the hippocampus every sixth consecutive section was used for the same staining. Free-floating sections were blocked with a mixture of 10% horse serum (HS) and 0.5% Triton X-100 in PBS for 1h at room temperature (RT) and incubated in a mixture of primary antibodies diluted in PBS +10% HS, followed by secondary fluorochrome-conjugated antibodies (Alexa-Fluor series, Invitrogen, Karlsruhe, Germany) in PBS for 2-3 h. Each step was followed by washing with PBS for 3x10 min at RT. For nestin, double-immunolabeling with other primary antibodies was performed in subsequent steps. Sections were mounted on Superfrost glass slides in Mowiol.

The primary and secondary antibodies used in this study are listed in Table 1. We used two antibodies against GFAP. The rabbit polyclonal antibody was employed to visualize radial glial processes over the entire period of dentate gyrus development (Forster et al. 2002;Weiss et al. 2003). As this antibody was not entirely specific for GFAP (as shown by western blotting, Suppl.Fig. 1E), we used the mouse monoclonal antibody directed against an epitope in the rod portion of GFAP to specifically immunolabel GFAP (Suppl.Fig. 1).

To secure comparability in developmental profiling of the different markers, tissue was processed and stained in parallel. Identical conditions were applied for microscopy and image processing. Images were acquired using a Zeiss Axioplan-2 Imaging microscope (Zeiss, Oberkochen, Germany) equipped with the following objectives: Plan-Apochromat 10x/0.45, Plan-Apochromat 20x/0.75, Plan-Neofluar 40x/1.30 Oil-DIC, Plan-Apochromat 63x/1.40 Oil, and captured with an Axiocam-Mrm digital camera (Zeiss). All figures show optical sections, which were obtained with a Zeiss ApoTome using structured illumination (Karadaglic 2008). In some cases, extended focus images are shown as indicated in the Figure Legends to better visualize the radial processes. These were calculated from z-stacks of optical sections using AxioVision software (Zeiss). Images were corrected for brightness and contrast with AxioVision and Photoshop-CS (Adobe, San Jose, USA) software.

BrdU Injection, Immunohistochemical Detection and Quantification of Marker Co-expression

Six NMRI mice received a single intraperitoneal (i.p.) injection of 50 μg 5-bromo-2-deoxyuridine (BrdU; Sigma, Munich, Germany) per gram (body weight) in 0.9% NaCl at P2 or P10, respectively, and tissue was taken at 6h, 12h and 24h post-injection (p.i.). Another ten NMRI mice were injected at P3 and tissue was taken 1d, 3d, 7d, 14d and 19d p.i. For immunohistochemistry, 50 μm vibratome sections were treated with 2M HCl at 37°C for 30 min and washed in 0.1M phosphate buffer (PB, pH 7.4) at RT. The sections were blocked in 0.1M PB containing 10% normal donkey serum, 1% Triton X-100 and 10% avidin for 1h, followed by incubation in a mixture of primary antibodies including rat anti-BrdU diluted in PB containing 10% biotin at 4°C. The sections were incubated with a rat IgG-specific biotin-conjugated antibody, followed by incubation for 2h with a mixture of fluorochrome-labeled avidin (AMCA-Avidin 1:200, biotin-avidin reagents from Vector Laboratories, Burlingame, CA/USA) and fluorochrome-conjugated secondary antibodies in PB. To quantify the colocalization of markers in BrdU-labeled cells, four sections from two animals were analyzed. 20 BrdU-positive cells from the molecular layer, granular layer and hilus (n=60 cells per section; n=240 cells per marker and timepoint) were randomly selected for unbiased counting and avoiding of double-counts, and expression of the different markers in these selected BrdU-positive cells was evaluated. Results are represented as mean ±SD. Statistical testing was carried out applying univariate ANOVA for the different time points, and Duncan and LSD for post-hoc comparisons.

For the reconstruction of nestin-positive processes, z-stacks of 16 optical sections throughout the rostrocaudal extent of the dentate gyrus spaced at 0.55μm were acquired with the 20x objective lens. First, a random sample of at least 75 labeled cells per timepoint was selected in the BrdU channel. Expression of nestin in these cells and the morphology of nestin-positive processes was analysed in all three dimensions using the individual z-sections. Processes of individual BrdU-labeled cells were traced using the Photoshop selection tool.

Primary Hippocampal Cell Culture and Immunocytochemistry

Hippocampi from six P2 NMRI mice and two hGFAP-eGFP mice were isolated and trypsinized in 450 μl Hanks' Balanced Salt Solution (HBSS) (Lonza, Basel, Switzerland) supplemented with trypsin-EDTA (Sigma) at 37°C for 10 min. The digestion was stopped by two short washes with 1 ml Dulbecco's Modified Eagle Medium (DMEM, 4.5 g/L glucose, Lonza). Thereafter, the tissue was dissociated in trituration medium as described (Bock and Herz 2003). 150 μl of this cell suspension were diluted in DMEM +4.5g/L glucose, 2 mM Glutamax, and 10% fetal calf serum. The cells were plated at a density of 12000/cm^2 on poly-D-lysine-coated coverslips and maintained in a 6.8% CO_2 atmosphere at 37°C. After 4h, the medium was replaced with fresh medium. 8h after plating the cells were fixed with 4% PFA for 20min and further analyzed by immunocytochemistry. Cells were permeabilized, blocked with PBS +10% HS +0.1% Triton-X-100 for 30 min and incubated with primary antibodies diluted in PBS +10% HS at 4°C overnight, followed by incubation with appropriate fluorochrome-conjugated secondary antibodies (Table 1). After mounting with Mowiol the cells were imaged as described above. Single- and double-labeled cells were counted using Photoshop and ImageJ (http://rsbweb.nih.gov/ij) processing software.

Preparation of Organotypic Hippocampal Slice Cultures and Time-Lapse Microscopy

Hippocampi from five heterozygous P7 GFAP-eGFP mice were dissected and cut into 150 μm-thick slices with a Mcllwain tissue chopper (Mickle Laboratories, Guildford, UK). The slices were transferred onto slice culture inserts (Millipore, Schwalbach, Germany), which were placed in a six-well plate with 1 ml/well nutrition medium containing 25% HS, 25% HBSS and 2 mM glutamine in Minimum Essential Medium (MEM, all from Invitrogen) adjusted to pH 7.2 and incubated in 5% CO_2 at 37°C. Time-lapse imaging was performed on

an Axiovert 200M inverted microscope (Zeiss) equipped with a CO_2- and heat-controlled stage incubator (Zeiss) using 475/440 nm excitation and 530/550 nm emission filters. Images were captured every 3 minutes for up to 21 hours using a 10x objective lens with OpenLab imaging software (Improvision, Coventry, UK). Data were analyzed using Adobe photoshop software. The red dots in Fig. 10H correspond to the positions of cell bodies, which were tracked in individual images captured every 15 min to determine the direction and mean speed of migrating cells.

Results

Time Course of Radial Glial Development in the Murine Dentate Gyrus

To visualize the temporal course of radial glial development in the murine dentate gyrus during the perinatal and early postnatal period we used a rabbit polyclonal antibody against GFAP (see Materials and Methods) which labels radial glial cells during the entire period of dentate gyrus development. At E16.5, the antibody immunostained the fibers of the primordial radial glial scaffold, which extend from the neuroepithelium of the ventricular zone near the prospective fimbria to the developing dentate gyrus (Fig. 1A,A'). Around birth, the radial fibers of the primordial scaffold were much reduced in number, while many immunolabeled cells with short processes covered the dentate area (Fig. 1B,B'). By P3, the primordial glial scaffold had disappeared, while processes of the now emerging secondary radial glial scaffold traversed the forming granule cell layer, projecting towards the molecular layer (Fig. 1C,C'). The radial morphology of this scaffold was fully developed during the second postnatal week (Fig. 1D,D',E,E') and gradually regressed thereafter, although it could still clearly be delineated at P21, when the development of the dentate gyrus is largely completed (Fig. 1F,F'). Cells that displayed a branched morphology of their radially oriented fibers (arrowheads, Fig. 1E',F') became increasingly apparent around P14, suggesting that a proportion of secondary radial glial cells transforms into astrocytes.

BLBP Immunostaining Distinguishes Between Primordial and Secondary Radial Glial Scaffold

BLBP is a small nucleocytoplasmic protein that is expressed by radial glial cells in different brain regions during development and in adult radial glia, including cerebellar Bergmann glia and retinal Müller cells (Pinto and Gotz 2007). At E16.5 and P0, BLBP was primarily detected in the prominent primary radial processes spanning the developing dentate gyrus (Fig. 2B, Suppl.Fig. 2A). This staining pattern closely resembles that of BLBP in neocortical radial glia (Fig. 2A). At P3, BLBP-positive cells with short processes were scattered over the dentate area (Fig. 2D1, Suppl.Fig. 2B). In cells of the postnatal secondary radial glial scaffold, however, BLBP immunoreactivity was largely confined to the somata and nuclei of secondary radial glial cells within the subgranular zone (Fig. 2C, arrow), whereas the radial processes, visualized by GFAP immunoreactivity, were only weakly labelled (arrowheads in Fig. 2D2). We also detected BLBP-immunoreactive cells whose cell bodies were positioned within the granular layer. These cells, presumably radial glial cells transforming into astroglia, extended characteristic branched processes towards the molecular layer (arrowheads, Fig. 2C,D3). Of note, the peak of BLBP immunoreactivity in the hilus and in the molecular layer, two astrocyte-enriched regions in the dentate gyrus, was observed in the first postnatal week (Supp.Fig. 2C), suggesting that BLBP labels, besides radial glial cells, immature astrocytes in the developing dentate gyrus.

Immunohistochemical Characterization of Radial Glial Maturation in the Dentate Gyrus

Our morphological analysis (Fig. 1) demonstrates that the secondary radial glial scaffold emerges around P3. To facilitate a better phenotypic characterization of radial glial maturation in the dentate gyrus we examined the spatiotemporal distribution of radial glial cells using

different molecular markers that have been shown to label radial glial cells in other brain regions (Bonfanti and Peretto 2007;Pinto and Gotz 2007;Rakic 2003). We assumed that the expression profile of different markers at sequential developmental time points would allow us to structure the continuous process of secondary radial glial formation and subsequent maturation into characteristic stages. Immunoreactivity against the intermediate filament protein nestin was strongest in the developing secondary radial glial scaffold (P3), declining thereafter (Fig. 3A). In hippocampal sections from 3-week old mice, nestin immunoreactivity was confined to the subgranular zone (Fig. 3A3), where it is expressed by radial glial-like progenitor cells (Filippov et al. 2003;Fukuda et al. 2003;Kempermann et al. 2004;Seri et al. 2004). In contrast to nestin, the intermediate filament protein vimentin was almost absent at P3 but prominently expressed in the fully developed secondary radial glial scaffold at P10 (Fig. 3B2). At P21, few radial glial cells (Fig. 3C, arrowhead) and astrocytes of the molecular layer expressed vimentin (Fig. 3B3), while many astrocytes of the hilar region remained vimentin-positive (Fig. 3C, arrow). Immunoreactivity against GFAP was prominent in radial glial fibers during the second and third postnatal week, whereas only few cells expressed GFAP at P3 (Fig. 2D1-3).

The astrocyte-specific glutamate-aspartate transporter (GLAST/EAAT1), a commonly used radial glial marker (Anthony and Heintz 2008; Hartfuss et al. 2001), was detected in the majority of cells in the proliferative zone of the hilus around birth and remained primarily expressed in radial glial cells until the third postnatal week (Fig. 4A). Coimmunostaining with the polyclonal GFAP antibody was used to visualize the radial processes (Fig. 4A), which was important for the identification of secondary radial glial cells based on morphological criteria. At P21, radial glial cells in the subgranular zone expressed GLAST (Fig. 4A4). Weak punctate GLAST immunostaining was also observed in astrocytes in the hilus and in the molecular layer (Fig. 4A5). The other astroglial glutamate transporter, GLT1 (EAAT2), was detected at late developmental stages (Fig. 4B1-3), where it was expressed both in radial glial cells and in astrocytes of the hilus and molecular layer (Fig. 4B4-5). No significant expression of the astroglial marker glutamine synthetase (GS) was detected in radial glial cells at all examined time points (Fig. 4C1-4), underlining that there are differences in the expression of marker proteins between secondary radial glial cells of the dentate gyrus and radial glia in other brain regions (Pinto and Gotz 2007).

The calcium-binding astrocytic protein S100-beta was detected in GFAP-positive cells with a radial glial appearance in the rat dentate gyrus (arrows, Supp.Fig. 3A-B, (Namba et al. 2005)). However, staining was not evident before P10 in mice, where its expression was confined to stellate-shaped astrocyte-like cells in the molecular layer, superficial granule cell layer and hilus (Suppl.Fig. 3C-D), confirming its usefulness as an astrocytic marker in the mouse (Ogata and Kosaka 2002; Raponi et al. 2007). Since many earlier studies on the development of the dentate gyrus have been performed in the rat, we compared the expression of several radial glial markers (nestin, vimentin, GFAP, GLAST, BLBP) in the developing dentate gyrus at representative time points (P3, P10, P21). Except for S100-beta we found no significant differences between rat and mouse (not shown).

The results of our immunohistochemical profiling of the secondary radial glial scaffold with a panel of antibodies against astroglial marker proteins are schematically summarized in Figure 5. The profile provides a framework for the analysis of its maturation in the developing dentate gyrus.

Formation and Proliferative Activity of the Secondary Radial Glial Scaffold

Shortly after birth, the majority of glial cells in the dentate area possess short non-radial processes, indicating that the primordial radial glial scaffold disappears while the secondary radial glial scaffold has not yet evolved (Fig. 1B-C,B'-C'). To follow the generation of early

secondary radial glial cells we birthdated proliferating precursor cells at P2 by injecting BrdU, and traced labeled cells by immunohistochemistry with antibodies against radial glial marker proteins. Since almost all BrdU-labeled cells expressed nestin for at least 24 hours (90.8 ±7.9%, n=127 cells 6h, 94.2±2.6%, n=128 cells 24h post-injection), we chose this marker for further analysis. Six hours after BrdU administration, the majority of BrdU-positive cells, which were scattered over the dentate area, displayed short nestin-positive processes (Fig. 6A). Twelve hours after injection, most of the labeled cells extended unipolar radial processes that were directed towards the granule cell layer (Fig. 6B). This indicates that a significant proportion of nestin-expressing dentate progenitor cells at early postnatal stages differentiate into secondary radial glia.

At this early stage of development, the proliferating cells are scattered all over the dentate area and in most cases do not have a radial appearance. As radial glial cells are the main precursor population of the adult dentate gyrus we wondered whether secondary radial glial cells might become the main precursor population once the scaffold has fully evolved. Therefore, we included P10 as a later stage of development. Again, most of the BrdU-labeled cells were nestin-positive six hours after injection (97.8 ±3.3%, n=78 cells) but, in contrast to P2, already extended unipolar radial processes through the granular layer (Fig. 6C). This indicates not only that secondary radial glial cells possess proliferative capacity, but also that they constitute the majority of proliferating cells at this later stage. The mitotic activity of secondary radial glia was confirmed by co-labeling of the M-phase marker phospho-histone H3 (pH3) and GFAP in secondary radial glial cells (Fig. 6E). Twelve hours after labeling, radial processes projecting into the granular layer were still detected in the majority of BrdU-positive cells (Fig. 6D). Similar results were obtained with vimentin as radial glial marker, although less BrdU-labeled cells were positive for vimentin at the chosen time intervals (data not shown).

In summary, secondary radial glial cells originate from the proliferative matrix in the dentate gyrus and constitute a main proportion of the precursor cell pool at later stages of dentate gyrus development.

BLBP as a Marker for Astroglial Transformation of Secondary Radial Glia in the Developing Dentate Gyrus

Previous studies have suggested that radial glia in different species and different brain regions directly transform into astroglia (Alves et al. 2002; Eckenhoff and Rakic 1984; Schmechel and Rakic 1979; Voigt 1989). BLBP is continuously expressed in the developing dentate gyrus and is detected in radial glia as well as in stellate cells with an astrocytic morphology (Fig. 2C-D, Suppl.Fig. 2). To clarify the usefulness of BLBP as a marker for astroglial transformation of secondary radial glial cells in the postnatal dentate gyrus we immunolabeled coronal sections of brains at different stages of dentate gyrus development with antibodies against BLBP and a second differentiation marker, based on our marker profile schematically summarized in Figure 5. Coimmunostaining of BLBP with the progenitor marker nestin was restricted to secondary radial glial cells (shown for P10, Fig. 7A,A’), whereas a colocalization of BLBP with the neuronal differentiation markers doublecortin and NeuN was not observed (Fig. 7B-C,B’-C’). On the other hand, BLBP-immunoreactive cells robustly expressed various astroglial markers predominantly in but not restricted to secondary radial glia at different developmental stages, including GLAST, vimentin and GFAP (Fig. 7D-F,D’-F’). Together these findings underline that BLBP is continuously expressed in the astroglial lineage while it is excluded from differentiating neurons in the developing dentate gyrus.

While many stellate-shaped cells in the astrocyte-enriched molecular layer (Ogata and Kosaka 2002) expressed BLBP at P10, almost no S100-beta immunoreactivity was detected at this stage (Fig. 7 G1). At P21, a proportion of cells was coimmunolabeled for both markers, with a decrease of BLBP and an increase of S100-beta immunoreactivity from the inner to the outer

regions of the molecular layer (Fig. 7 G2). In the adult dentate gyrus, however, almost no co-localization was detectable, with S100-beta being strongly expressed in the molecular layer and hilus, whereas BLBP was confined to the subgranular zone (Fig. 7 G3). Thus, the developmental time course of BLBP-S100-beta co-expression reflects the maturation of BLBP-positive cells into S100-beta-positive astrocytes, supporting BLBP's role as a transient marker of astroglial differentiation in the dentate gyrus. In summary, our results indicate that BLBP is expressed by secondary radial glia and differentiating astroglial cells in the dentate gyrus.

We also quantified the degree of overlap between BLBP and the different astroglial markers using an in vitro model of acutely dissociated postnatal hippocampal cultures (Suppl.Fig. 4). Comparable cell culture models have been used to characterize precursor cell pools in different brain regions (Culican et al. 1990; Hartfuss et al. 2001; Stipursky and Gomes 2007). Almost all of the cultured neurons expressed the granule cell marker Prox1 (Suppl.Fig. 4A-B). Quantitative double-immunocytochemistry of freshly dissociated hippocampal cells that were cultured for eight hours demonstrated an almost complete colocalization of the astroglial differentiation markers GLAST, vimentin, GFAP and S100-beta with BLBP. On the other hand, cells positive for each of these markers represented subfractions of the BLBP-positive population. This underlines our observation in immunolabeled brain sections that GLAST, vimentin, GFAP and S100-beta label astroglial cells at different maturation stages, while BLBP immunoreactivity characterizes the majority of immature astroglial cells. 6% of all cells co-expressed BLBP and the marker of mature neurons, NeuN (Suppl.Fig. 4C). These cells might correspond to the NeuN-positive proliferating astrocytes that were recently described in primary brain cultures (Darlington et al. 2007).

Astrocytic Transformation of Secondary Radial Glia during Late Astrogliogenesis

We next used BLBP as a molecular marker to monitor the astroglial transformation of secondary radial glia by correlating the morphological changes with the marker signature of BLBP-immunoreactive cells over time at late stages of development. We focused our analysis on BLBP-positive cells within the granule cell layer and the inner molecular layer, which presumably represent transforming secondary radial glia. Nestin+ BLBP+ cells, which were rarely detectable after the second postnatal week, extended nestin-positive, unbranched radial processes through the granule cell layer (arrowheads, Fig. 8A). These cells, which also expressed GFAP, were confined to the subgranular zone and probably correspond to the putative stem cells of adult neurogenesis in the dentate gyrus (Garcia et al. 2004;Kempermann et al. 2004;Seri et al. 2004;Seri et al. 2001). At P10, many radial glial cells were coimmunolabeled by antibodies against GFAP and BLBP (Fig. 8B1). We occasionally found BLBP+ GFAP+ cells whose somata were located within the inner part of the granule cell layer (Fig. 8B1, arrowheads). At P21, double-labeled cells within the granular layer were found more frequently and were distributed over its entire width. Most of these cells extended branched radial processes (Fig. 8B2, arrowheads) and lacked nestin immunoreactivity (Fig. 8A2, arrowheads). The processes of GFAP+ BLBP+ cells in the outer third of the granular layer frequently displayed a complex arborisation, resembling star-shaped astrocytes (Fig. 8B2,Suppl.Fig. 5). Triple-immunostaining demonstrated that these cells, which presumably correspond to advanced stages of astroglial differentiation, were also weakly immunoreactive for GLAST (Fig. 8C). Altogether, our results suggest that BLBP and GLAST serve as markers of radial glial-astrocytic transformation in the dentate gyrus, as has been shown for other brain regions (Barry and McDermott 2005;Hartfuss et al. 2001;Shibata et al. 1997).

The described morphological changes and spatial relocalization of GFAP-BLBP-GLAST triple-immunoreactive cells suggested a directed migration process of immature astrocytes from the inner part of the granular layer towards the molecular layer. In line with this

conclusion, we occasionally found BLBP-immunoreactive stellate-shaped cells expressing the astrocyte-specific marker protein S100-beta in the innermost part but not in more distant regions of the molecular layer (Fig. 7G2). These cells probably represent terminally differentiating astrocytes, because the majority of S100-beta-positive cells in the molecular layer did not express BLBP. Thus, it can be concluded that BLBP is primarily expressed in immature astroglial cells that downregulate BLBP late in the transformation process. These data suggest that transforming BLBP-positive secondary radial glial cells migrate through the granule cell layer to differentiate into astrocytes and populate the molecular layer. A model of the proposed astroglial differentiation and migration in the developing dentate gyrus is described in Figure 9.

Direct Visualization of Astrocytic Precursor Cell Migration by Time-Lapse Microscopy

To directly visualize the proposed astrocyte precursor migration in the developing dentate gyrus, we performed time-lapse microscopy on organotypic hippocampal slice cultures from transgenic mice expressing eGFP under the control of the hGFAP promoter (Fig. 10). These mice express eGFP in many cells that display morphological and electrophysiological characteristics of astrocytes or glial precursor cells (Nolte et al. 2001). Importantly, no colocalization of the neuronal markers Prox1 (Fig. 10B,B') and NeuN (Fig. 10C,C') with eGFP fluorescence at P7 was detected in the dentate gyrus. Instead, the green fluorescent signal colocalized with the precursor cell marker nestin (Fig. 10A,A') and different markers that characterize the astroglial lineage (Fig. 10D-F,D'-F'). This was confirmed by quantitative immunocytochemistry of acutely dissociated hippocampal cells (Suppl.Fig. 6), thus validating this mouse model for our purpose to study glial migration in the developing dentate gyrus. A typical eGFP-positive BLBP-expressing cell is shown in Figure 10G, which corresponds to an immature astroglial cell within the granule cell layer (arrow).

After recovery at P7, acute slices were observed by fluorescence microscopy for up to 21 hr. Most of the fluorescent cells were located to the hilar region and in the molecular layer, whereas the granule cell layer appeared as a fluorescent-poor area (Fig. 10H). During the imaging period, many eGFP-fluorescent cells did not display a directed movement, although many of them moved back and forth while remaining stationary. However, most of the migrating fluorescent cells moved radially outward, starting from the hilus, the incipient subgranular zone or from within the granule cell layer (dotted arrows in Fig. 10H). Of note, cells migrating in the opposite direction were observed as well; occasionally, cells started to migrate outwards and later reverted their migration direction towards the hilus. We observed that the fluorescent cells utilized at least two different modes of migration: Cell 1 extended an unbranched radial process along which its soma (Fig. 10I, arrow) translocated towards the molecular layer. Cell 2 displayed a multipolar morphology during the migration process (not shown). This second migratory mode was observed in approx. 10% of all radially outward-moving cells. The velocity profile of cell 1 (Suppl.Fig. 7) demonstrated that the bulk of the migration distance was covered within a short period of 30 min, where it reached a maximum mean cell speed of almost 70 μm/hr. In conclusion, time-lapse imaging in acute hippocampal slices provides evidence for a directed migration of astroglial cells during dentate gyrus development.

Comparison of Astroglial Transformation of Secondary Radial Glial cells with Astrogliogenesis during Early Stages of Dentate Gyrus Development

To compare the astroglial transformation of secondary radial glia during later stages of development with the differentiation of astroglial cells in the early postnatal dentate gyrus, where non-radial cells form the majority of precursor cells, we labeled proliferating cells at P3 by a single BrdU injection. We examined the tissue at consecutive timepoints after injection and followed the expression of the different glial markers in BrdU-labeled cells (Fig. 11A). Birthdating was performed at day P3 because at this stage a maximum of cytogenesis in the

dentate gyrus is observed (Suppl.Fig. 8A) and a significant proportion of the labeled cells differentiate into astrocytes (Altman and Bayer 1990a;Cowan et al. 1980;Reznikov 1991).

Most of the labeled cells became confined to the granular layer at later stages of development (Fig. 11C), where the majority differentiated into NeuN-positive neurons (Suppl.Fig. 8B). Since we were interested in the glial differentiation of precursor cells, we focused our analysis on BrdU-positive cells that were localized to the astrocyte-enriched polymorphic and molecular layers of the dentate gyrus. As the majority of hilar mossy cells and dentate interneurons are born prenatally (Li et al. 2008;Soriano et al. 1986;Soriano et al. 1989) and because only a small fraction of labelled cells in the molecular layer was positive for the marker of oligodendrocyte precursors NG2 (Nishiyama et al. 2009) 24h after birthdating (Suppl.Fig. 4C, see also (Reznikov 1991)), it can be assumed that a significant proportion of the analyzed cells belong to the astroglial lineage.

The majority (87.0 ±2.1%) of the BrdU-labeled cells expressed nestin 24h after birthdating at P3. In the further course of development the proportion of nestin-positive cells that had been labelled with BrdU at P3 steadily declined to 7.7 ±4.1% at P22 (Fig. 11A), which is in accordance with a role for nestin as a marker of progenitor cells in the developing dentate gyrus. Most of the remaining nestin-immunoreactive BrdU-positive cells were found in the subgranular zone (Fig. 11E) and might represent slowly-proliferating, self-renewing progenitor cells. Some BrdU-labeled cells exhibited GFAP immunoreactivity at P4 (10.6 ±4.5%). The rate of GFAP-positive, BrdU-labeled cells considerably increased to 30.5 ±4.7% one week after the BrdU pulse and 53.5 ±8.0% at P16, but did not significantly increase further (62.5 ±2.0% at P22). The first BrdU+ cells expressing S100-beta, a marker protein for mature astrocytes in mice, were detected one week after the injection (11.9 ±3.3% at P10). Its expression in labelled cells steadily increased to 35.8 ±4.3% at P22 (Fig. 11A). Cells that were positive for both BrdU and BLBP at P4 amounted to 30.8 ±3.6% of all birthdated cells. The percentage of BLBP-positive BrdU-labeled cells slightly increased during the first week after birthdating to 42.0% ±3.0% at P10 and moderately declined to 29.7 ±4.8% (P16) and 29.4 ±2,8% at P22 (Fig. 11A), suggesting that BLBP is expressed during a prolonged period in differentiating glial cells of the dentate gyrus. This is supported by the localization of BrdU-labeled BLBP-expressing cells at P22 in the hilus and molecular layer (Fig. 11G). Our analysis reflects the changing astroglial marker profile of differentiating precursor cells during astrogliogenesis in the dentate gyrus.

These results suggest that the marker expression of transforming secondary radial glial cells closely resembles the immunohistochemical maturation process of early-generated astroglial cells, with the notable exception of GFAP. This marker is upregulated only late during early astrogliogenesis, whereas it characterizes the transforming secondary radial glia from the beginning.

Discussion

Previous studies have used classical neuroanatomical techniques to describe the formation of the secondary radial glial scaffold during the development of the dentate gyrus (Eckenhoff and Rakic 1984; Rickmann et al. 1987; Sievers et al. 1992; Woodhams et al. 1981). Here, we combined immunolabeling against radial glial and glial markers with the evaluation of the morphology and spatial location of immunoreactive cells over time. This allowed us to establish a comprehensive spatial and temporal expression profile of the secondary radial glial scaffold (Figure 5), which provides a useful framework for the analysis of mouse mutants with defects in dentate morphogenesis or radial glial assembly. This will facilitate the identification of mechanisms that are important for radial glial maturation and differentiation.

By combining antigenic phenotyping with BrdU birthdating analyses, we demonstrate that the secondary radial glia are derived from the precursor cell pool in the dentate proliferative matrix and function as progenitor cells themselves at later stages of development. Our results indicate that the transformation of secondary radial glial cells into astrocytes involves a transitional immature cell population, which is characterized by expression of BLBP, GFAP and GLAST and migrates through the granule cell layer. By comparing this transformation of secondary radial glial cells at late stages of dentate gyrus development with the astroglial differentiation of early-born precursor cells we show that both populations undergo similar immunohistochemical maturation stages. Finally, we employ time-lapse microscopy of acute hippocampal slice cultures from hGFAP-eGFP transgenic mice to provide direct evidence for a radial migration mode of astroglial-committed differentiating cells into the molecular layer of the dentate gyrus.

Precursor Cell Functions of the Secondary Radial Glial Scaffold

Since radial glial cells function as progenitors in other parts of the developing brain and in the adult dentate gyrus, we questioned whether a similar function could be ascribed to the secondary radial glia during dentate development. At P2, most proliferating cells were dispersed over the entire dentate area and initially did not display the morphological characteristics of radial glia, although the majority developed nestin-positive radial processes later on. This demonstrates that secondary radial glial cells are derived from precursor cells in the dentate area but do not constitute a considerable part of the precursor pool at this early stage of development. In contrast, most of the proliferating cells at P10 displayed morphological characteristics of radial glial cells from the beginning and were located in the subgranular zone. These data suggest that non-radial precursor cells in the early postnatal dentate gyrus give rise to secondary radial glial cells, which in turn are the main precursor cells at later stages of dentate morphogenesis.

Transformation of Secondary Radial Glia into Astrocytes

Our results (Figure 9) provide evidence for a morphogenetic transformation of radial glia (Alves et al. 2002;Eckenhoff and Rakic 1984;Hatten 1999;Schmechel and Rakic 1979;Voigt 1989) while translocating through the granule cell layer to populate the molecular layer. During the third postnatal week the secondary radial glia undergoes considerable morphological changes, leading to a gradual disassembly of the evenly arranged scaffold. At P10, BLBP-positive somata are located in the subgranular zone or in the innermost granule cell layer, where they extend long unbranched, evenly arranged GFAP-positive processes through the granule cell layer. At later stages, GFAP-BLBP double-labeled cells are found inside the granule layer, extending branched processes towards the molecular layer. While the few remaining BLBP-immunoreactive cells that are confined to the subgranular zone still express nestin, cells that have translocated into the granule cell layer become nestin negative, which indicates a more mature state. Between superficial regions of the granule cell layer and the inner molecular layer, a subset of BLBP-positive cells lose their GFAP immunoreactiviy. This is in accordance with the finding that only a subset of mature astrocytes in the hippocampus express GFAP (Ogata und Kosaka, 2002). While BLBP is strongly expressed in transforming cells within the granule cell layer, its expression gradually decreases in cells that have reached the molecular layer. This leads to a gradient of BLBP-immunoreactive cells in the inner molecular layer and S100-beta positive cells in superficial regions of the molecular layer with a population of double-labeled cells in between. In adult animals, however, S100-beta-positive astrocytes of the molecular layer did not express BLBP. A similar downregulation of BLBP expression in translocating radial glia upon their transformation into mature astrocytes has also been described for the developing spinal cord (Barry and McDermott 2005) and for cortical progenitor cultures under gliogenic conditions (Stipursky and Gomes 2007).

Together, it can be concluded that in the developing dentate gyrus BLBP is expressed in immature astroglial cells that downregulate BLBP once they have terminated the differentiation process (Fig. 9), and that secondary radial glial cells are a major source of astrocytes during late stages of dentate gyrus development. However, it should be noted that many differentiating BLBP-positive cells can be found in the subpial region around birth (Suppl.Fig. 2A,B), when cytogenesis in the dentate gyrus is high. This implies the existence of an additional subpial pool of astroglial progenitors at earlier developmental stages, similar to the recently described transient subpial neurogenic zone in the dentate gyrus (Li et al. 2009).

By birthdating proliferating cells in the dentate gyrus at P3 and following their maturation with immunohistochemical markers (Fig. 11A) we found a largely similar course of astroglial differentiation of these early precursors as compared with the transformation of secondary radial glial cells into astrocytes at later stages. In both cases nestin immunoreactivity is quickly downregulated, BLBP expression remains constant over a prolonged period and S100-beta only emerges at late stages. A notable difference concerns GFAP, which is upregulated late during the astroglial maturation of the early precursor population, while it is already expressed in secondary radial glia after the first postnatal week. It is likely that the BrdU-labeled NG2-immunoreactive cells detected at P4 account for at least some of the oligodendrocytes in the molecular layer, although we cannot exclude that a proportion of them might differentiate into other cell types, including astrocytes (Hewett 2009;Nishiyama et al. 2009).

Transformation of Radial Glia and Glial Migration in the Postnatal Dentate Gyrus in Comparison with the SVZ

By using organotypic slice cultures from hGFAP-eGFP mice we were able to directly visualize the proposed migration of glial cells in the developing dentate gyrus. The observed predominant migration mode of GFP-fluorescent cells resembled the somal translocation of early-born neurons in the neocortex. The maximal speed of 70 μm/hr of migrating GFP-positive cells is comparable to that of translocating neurons (Nadarajah et al. 2001) or migrating SVZ glioblasts (Kakita and Goldman 1999) and would allow for a rapid translocation through the granule cell layer. Other migration modes were less frequently observed. In addition to the outward radial migration, we also noted an inward movement of glial cells towards the hilus in the dentate gyrus.

The hippocampal subgranular zone (SGZ) and the subventricular zone (SVZ) adjacent to the forebrain lateral ventricles are germinative layers where active neurogenesis persists into adulthood (Ming and Song 2005). Both regions undergo considerable postnatal modifications during the first two weeks after birth in rodents, which might be important for the maintenance of a stem cell niche in an otherwise mature brain environment (Peretto et al. 2005). Morphological and functional differences between both adult proliferative zones include the absence of ventricular contact of the SGZ and the long-distance migration of SVZ-derived neuroblasts into the olfactory bulb as opposed to the apposition of newly generated neurons in the SGZ close to their site of origin (Lois and Alvarez-Buylla 1994; Zhao et al. 2006). However, the most striking difference between both proliferative regions concerns the postnatal assembly and persistence into adulthood of a secondary radial glial scaffold in the SGZ (Kempermann et al. 2004; Seri et al. 2004; Seri et al. 2001; Steiner et al. 2004). In contrast, the radial glia of the early postnatal SVZ almost completely disappears and is replaced by adult SVZ astrocytes, which form glial tubes that are important for chain migration of neuroblasts and can function as stem cells themselves (Bonfanti and Peretto 2007; Doetsch et al. 1999; Peretto et al. 2005).

Despite these differences, a comparison of the radial glia to astrocyte transition in both regions reveals some interesting similarities. In the SVZ, radial glia is abundant around birth and almost disappears during the first two postnatal weeks (Tramontin et al. 2003), which is paralleled by its transformation into astrocytes. Similarly, immature astrocytes derived from secondary

radial glia in the dentate gyrus undergo a morphogenetic transformation and translocate through the granule cell layer to populate the molecular layer. In both regions, the transition of transforming radial glia involves an outward migration, and glial cells of different developmental stages coexist, with an increase of mature forms at later time points. As in the dentate gyrus, migration in the SVZ is accompanied by the progressive acquisition of an increasingly complex branching pattern of transforming radial glia and a change in intermediate filament protein expression (Alves et al. 2002; Peretto et al. 2005). However, despite these parallels, it seems that the astrocytic transformation of radial glia in the developing SVZ and of secondary radial glia in the dentate gyrus serve distinct functions in both regions.

Supplementary Material

Refer to Web version on PubMed Central for supplementary material.

Acknowledgments

We thank Jonathan Göldner for excellent technical assistance, Helmut Kettenmann (Max-Delbrück-Center, Berlin-Buch, Germany) for kindly providing the hGFAP-eGFAP mice, Elly Hol (Department of Astrocyte Biology &Neurodegeneration, Netherlands Institute for Neuroscience, Amsterdam) for discussion, Manfred Olschewski (Institute of Medical Biometry und Statistics, University of Freiburg, Germany) for help with the statistical analysis, Dirk Junghans (Institute of Anatomy and Cell Biology, University of Freiburg) for critical reading of the manuscript, and Hubert E. Blum (Department of Medicine II, University Hospital Freiburg, Germany) for scientific support. The monoclonal antibodies Rat-401 (developed by S. Hockfield) and 40E-C (developed by A. Alvarez-Buylla) were obtained from the Developmental Studies Hybridoma Bank developed under the auspices of the NICHD and maintained by The University of Iowa, Department of Biological Sciences, Iowa City, IA 52242, USA. This study was supported by the Deutsche Forschungsgemeinschaft (grants BO1806/2-1 to H.B., SFB780-B5 to J.H., M.F. and H.B., MA2410/1-2 to P.M., and SFB TR3-C1 to A.D.) and the Humboldt Foundation (J.H.). M.F. was supported by the Hertie Foundation.

References

Altman J, Bayer SA. Migration and distribution of two populations of hippocampal granule cell precursors during the perinatal and postnatal periods. J Comp Neurol 1990a;301(3):365–81. [PubMed: 2262596]

Altman J, Bayer SA. Mosaic organization of the hippocampal neuroepithelium and the multiple germinal sources of dentate granule cells. J Comp Neurol 1990b;301(3):325–42. [PubMed: 2262594]

Alves JA, Barone P, Engelender S, Froes MM, Menezes JR. Initial stages of radial glia astrocytic transformation in the early postnatal anterior subventricular zone. J Neurobiol 2002;52(3):251–65. [PubMed: 12210108]

Anthony TE, Heintz N. Genetic lineage tracing defines distinct neurogenic and gliogenic stages of ventral telencephalic radial glial development. Neural Develop 2008;3(1):30.

Barry D, McDermott K. Differentiation of radial glia from radial precursor cells and transformation into astrocytes in the developing rat spinal cord. Glia 2005;50(3):187–97. [PubMed: 15682427]

Bignami A, Dahl D. Astrocyte-specific protein and neuroglial differentiation. An immunofluorescence study with antibodies to the glial fibrillary acidic protein. J Comp Neurol 1974;153(1):27–37. [PubMed: 4593733]

Bock HH, Herz J. Reelin activates Src family tyrosine kinases in neurons. Curr Biol 2003;13(1):18–26. [PubMed: 12526740]

Bonfanti L, Peretto P. Radial glial origin of the adult neural stem cells in the subventricular zone. Prog Neurobiol 2007;83(1):24–36. [PubMed: 17196731]

Cowan WM, Stanfield BB, Kishi K. The development of the dentate gyrus. Curr Top Dev Biol 1980;15 (Pt 1):103–57. Chapter 5. [PubMed: 6778660]

Culican SM, Baumrind NL, Yamamoto M, Pearlman AL. Cortical radial glia: identification in tissue culture and evidence for their transformation to astrocytes. J Neurosci 1990;10(2):684–92. [PubMed: 2303868]

Darlington PJ, Goldman JS, Cui QL, Antel JP, Kennedy TE. Widespread immunoreactivity for neuronal nuclei in cultured human and rodent astrocytes. J Neurochem. 2007

Doetsch F, Caille I, Lim DA, Garcia-Verdugo JM, Alvarez-Buylla A. Subventricular zone astrocytes are neural stem cells in the adult mammalian brain. Cell 1999;97(6):703–16. [PubMed: 10380923]

Eckenhoff MF, Rakic P. Radial organization of the hippocampal dentate gyrus: a Golgi, ultrastructural, and immunocytochemical analysis in the developing rhesus monkey. J Comp Neurol 1984;223(1): 1–21. [PubMed: 6707248]

Feng L, Hatten ME, Heintz N. Brain lipid-binding protein (BLBP): a novel signaling system in the developing mammalian CNS. Neuron 1994;12(4):895–908. [PubMed: 8161459]

Filippov V, Kronenberg G, Pivneva T, Reuter K, Steiner B, Wang LP, Yamaguchi M, Kettenmann H, Kempermann G. Subpopulation of nestin-expressing progenitor cells in the adult murine hippocampus shows electrophysiological and morphological characteristics of astrocytes. Mol Cell Neurosci 2003;23(3):373–82. [PubMed: 12837622]

Forster E, Tielsch A, Saum B, Weiss KH, Johanssen C, Graus-Porta D, Muller U, Frotscher M. Reelin, Disabled 1, and beta 1 integrins are required for the formation of the radial glial scaffold in the hippocampus. Proc Natl Acad Sci U S A 2002;99(20):13178–83. Epub 2002 Sep 20. [PubMed: 12244214]

Frotscher, M.; Seress, L. Morphological Development of the Hippocampus.. In: Per Andersen, RM.; Amaral, David; Bliss, Tim; O'Keefe, John, editors. The Hippocampus Book. Oxford University Press; New York: 2007. p. 872

Fukuda S, Kato F, Tozuka Y, Yamaguchi M, Miyamoto Y, Hisatsune T. Two Distinct Subpopulations of Nestin-Positive Cells in Adult Mouse Dentate Gyrus. J Neurosci 2003;23(28):9357–9366. [PubMed: 14561863]

Gage FH, Kempermann G, Palmer TD, Peterson DA, Ray J. Multipotent progenitor cells in the adult dentate gyrus. J Neurobiol 1998;36(2):249–66. [PubMed: 9712308]

Garcia AD, Doan NB, Imura T, Bush TG, Sofroniew MV. GFAP-expressing progenitors are the principal source of constitutive neurogenesis in adult mouse forebrain. Nat Neurosci 2004;7(11):1233–41. Epub 2004 Oct 24. [PubMed: 15494728]

Hall AC, Mira H, Wagner J, Arenas E. Region-specific effects of glia on neuronal induction and differentiation with a focus on dopaminergic neurons. Glia 2003;43(1):47–51. [PubMed: 12761866]

Hartfuss E, Galli R, Heins N, Gotz M. Characterization of CNS precursor subtypes and radial glia. Dev Biol 2001;229(1):15–30. [PubMed: 11133151]

Hatten ME. Central nervous system neuronal migration. Annu Rev Neurosci 1999;22:511–39. [PubMed: 10202547]

Hewett JA. Determinants of regional and local diversity within the astroglial lineage of the normal central nervous system. J Neurochem 2009;110(6):1717–1736. [PubMed: 19627442]

Kakita A, Goldman JE. Patterns and dynamics of SVZ cell migration in the postnatal forebrain: monitoring living progenitors in slice preparations. Neuron 1999;23(3):461–72. [PubMed: 10433259]

Karadaglic D. Image formation in conventional brightfield reflection microscopes with optical sectioning property via structured illumination. Micron 2008;39(3):302–10. [PubMed: 18024142]

Kempermann G, Jessberger S, Steiner B, Kronenberg G. Milestones of neuronal development in the adult hippocampus. Trends Neurosci 2004;27(8):447–52. [PubMed: 15271491]

Kriegstein AR, Gotz M. Radial glia diversity: a matter of cell fate. Glia 2003;43(1):37–43. [PubMed: 12761864]

Kurtz A, Zimmer A, Schnutgen F, Bruning G, Spener F, Muller T. The expression pattern of a novel gene encoding brain-fatty acid binding protein correlates with neuronal and glial cell development. Development 1994;120(9):2637–49. [PubMed: 7956838]

Li G, Berger O, Han SM, Paredes M, Wu NC, Pleasure SJ. Hilar Mossy Cells Share Developmental Influences with Dentate Granule Neurons. Dev Neurosci 2008;30(4):255–261. [PubMed: 17960053]

Li G, Kataoka H, Coughlin SR, Pleasure SJ. Identification of a transient subpial neurogenic zone in the developing dentate gyrus and its regulation by Cxcl12 and reelin signaling. Development 2009;136 (2):327–35. [PubMed: 19103804]

Lois C, Alvarez-Buylla A. Long-distance neuronal migration in the adult mammalian brain. Science 1994;264(5162):1145–8. [PubMed: 8178174]

Martin LA, Tan SS, Goldowitz D. Clonal architecture of the mouse hippocampus. J Neurosci 2002;22 (9):3520–30. [PubMed: 11978829]

Ming GL, Song H. Adult neurogenesis in the mammalian central nervous system. Annu Rev Neurosci 2005;28:223–50. [PubMed: 16022595]

Nadarajah B, Brunstrom JE, Grutzendler J, Wong RO, Pearlman AL. Two modes of radial migration in early development of the cerebral cortex. Nat Neurosci 2001;4(2):143–50. [PubMed: 11175874]

Nadarajah B, Parnavelas JG. Modes of neuronal migration in the developing cerebral cortex. Nat Rev Neurosci 2002;3(6):423–32. [PubMed: 12042877]

Namba T, Mochizuki H, Onodera M, Mizuno Y, Namiki H, Seki T. The fate of neural progenitor cells expressing astrocytic and radial glial markers in the postnatal rat dentate gyrus. Eur J Neurosci 2005;22(8):1928–41. [PubMed: 16262632]

Nishiyama A, Komitova M, Suzuki R, Zhu X. Polydendrocytes (NG2 cells): multifunctional cells with lineage plasticity. Nat Rev Neurosci 2009;10(1):9–22. [PubMed: 19096367]

Nolte C, Matyash M, Pivneva T, Schipke CG, Ohlemeyer C, Hanisch UK, Kirchhoff F, Kettenmann H. GFAP promoter-controlled EGFP-expressing transgenic mice: a tool to visualize astrocytes and astrogliosis in living brain tissue. Glia 2001;33(1):72–86. [PubMed: 11169793]

Ogata K, Kosaka T. Structural and quantitative analysis of astrocytes in the mouse hippocampus. Neuroscience 2002;113(1):221–33. [PubMed: 12123700]

Peretto P, Giachino C, Aimar P, Fasolo A, Bonfanti L. Chain formation and glial tube assembly in the shift from neonatal to adult subventricular zone of the rodent forebrain. J Comp Neurol 2005;487(4): 407–27. [PubMed: 15906315]

Pinto L, Gotz M. Radial glial cell heterogeneity--The source of diverse progeny in the CNS. Prog Neurobiol 2007;83(1):2–23. [PubMed: 17580100]

Rakic P. Elusive radial glial cells: historical and evolutionary perspective. Glia 2003;43(1):19–32. [PubMed: 12761862]

Raponi E, Agenes F, Delphin C, Assard N, Baudier J, Legraverend C, Deloulme JC. S100B expression defines a state in which GFAP-expressing cells lose their neural stem cell potential and acquire a more mature developmental stage. Glia 2007;55(2):165–77. [PubMed: 17078026]

Reznikov KY. Cell proliferation and cytogenesis in the mouse hippocampus. Adv Anat Embryol Cell Biol 1991;122:1–74. [PubMed: 1927657]

Rickmann M, Amaral DG, Cowan WM. Organization of radial glial cells during the development of the rat dentate gyrus. J Comp Neurol 1987;264(4):449–79. [PubMed: 3680638]

Schmechel DE, Rakic P. A Golgi study of radial glial cells in developing monkey telencephalon: morphogenesis and transformation into astrocytes. Anat Embryol (Berl) 1979;156(2):115–52. [PubMed: 111580]

Seri B, Garcia-Verdugo JM, Collado-Morente L, McEwen BS, Alvarez-Buylla A. Cell types, lineage, and architecture of the germinal zone in the adult dentate gyrus. J Comp Neurol 2004;478(4):359–78. [PubMed: 15384070]

Seri B, Garcia-Verdugo JM, McEwen BS, Alvarez-Buylla A. Astrocytes give rise to new neurons in the adult mammalian hippocampus. J Neurosci 2001;21(18):7153–60. [PubMed: 11549726]

Shapiro LA, Korn MJ, Shan Z, Ribak CE. GFAP-expressing radial glia-like cell bodies are involved in a one-to-one relationship with doublecortin-immunolabeled newborn neurons in the adult dentate gyrus. Brain Res 2005;1040(1-2):81–91. [PubMed: 15804429]

Shibata T, Yamada K, Watanabe M, Ikenaka K, Wada K, Tanaka K, Inoue Y. Glutamate transporter GLAST is expressed in the radial glia-astrocyte lineage of developing mouse spinal cord. J Neurosci 1997;17(23):9212–9. [PubMed: 9364068]

Sievers J, Hartmann D, Pehlemann FW, Berry M. Development of astroglial cells in the proliferative matrices, the granule cell layer, and the hippocampal fissure of the hamster dentate gyrus. J Comp Neurol 1992;320(1):1–32. [PubMed: 1401238]

Soriano E, Cobas A, Fairen A. Asynchronism in the neurogenesis of GABAergic and non-GABAergic neurons in the mouse hippocampus. Brain Res 1986;395(1):88–92. [PubMed: 3022890]

Soriano E, Cobas A, Fairen A. Neurogenesis of glutamic acid decarboxylase immunoreactive cells in the hippocampus of the mouse. II: Area dentata. J Comp Neurol 1989;281(4):603–11. [PubMed: 2708584]

Stanfield BB, Cowan WM. The development of the hippocampus and dentate gyrus in normal and reeler mice. J Comp Neurol 1979;185(3):423–59. [PubMed: 86549]

Steiner B, Kronenberg G, Jessberger S, Brandt MD, Reuter K, Kempermann G. Differential regulation of gliogenesis in the context of adult hippocampal neurogenesis in mice. Glia 2004;46(1):41–52. [PubMed: 14999812]

Stipursky J, Gomes FC. TGF-beta1/SMAD signaling induces astrocyte fate commitment in vitro: implications for radial glia development. Glia 2007;55(10):1023–33. [PubMed: 17549683]

Tramontin AD, Garcia-Verdugo JM, Lim DA, Alvarez-Buylla A. Postnatal development of radial glia and the ventricular zone (VZ): a continuum of the neural stem cell compartment. Cereb Cortex 2003;13(6):580–7. [PubMed: 12764031]

Voigt T. Development of glial cells in the cerebral wall of ferrets: direct tracing of their transformation from radial glia into astrocytes. J Comp Neurol 1989;289(1):74–88. [PubMed: 2808761]

Weiss KH, Johanssen C, Tielsch A, Herz J, Deller T, Frotscher M, Forster E. Malformation of the radial glial scaffold in the dentate gyrus of reeler mice, scrambler mice, and ApoER2/VLDLR-deficient mice. J Comp Neurol 2003;460(1):56–65. [PubMed: 12687696]

Woodhams PL, Basco E, Hajos F, Csillag A, Balazs R. Radial glia in the developing mouse cerebral cortex and hippocampus. Anat Embryol (Berl) 1981;163(3):331–43. [PubMed: 7340560]

Zhao C, Teng EM, Summers RG Jr. Ming GL, Gage FH. Distinct morphological stages of dentate granule neuron maturation in the adult mouse hippocampus. J Neurosci 2006;26(1):3–11. [PubMed: 16399667]

Zhao S, Chai X, Forster E, Frotscher M. Reelin is a positional signal for the lamination of dentate granule cells. Development 2004;131(20):5117–25. [PubMed: 15459104]

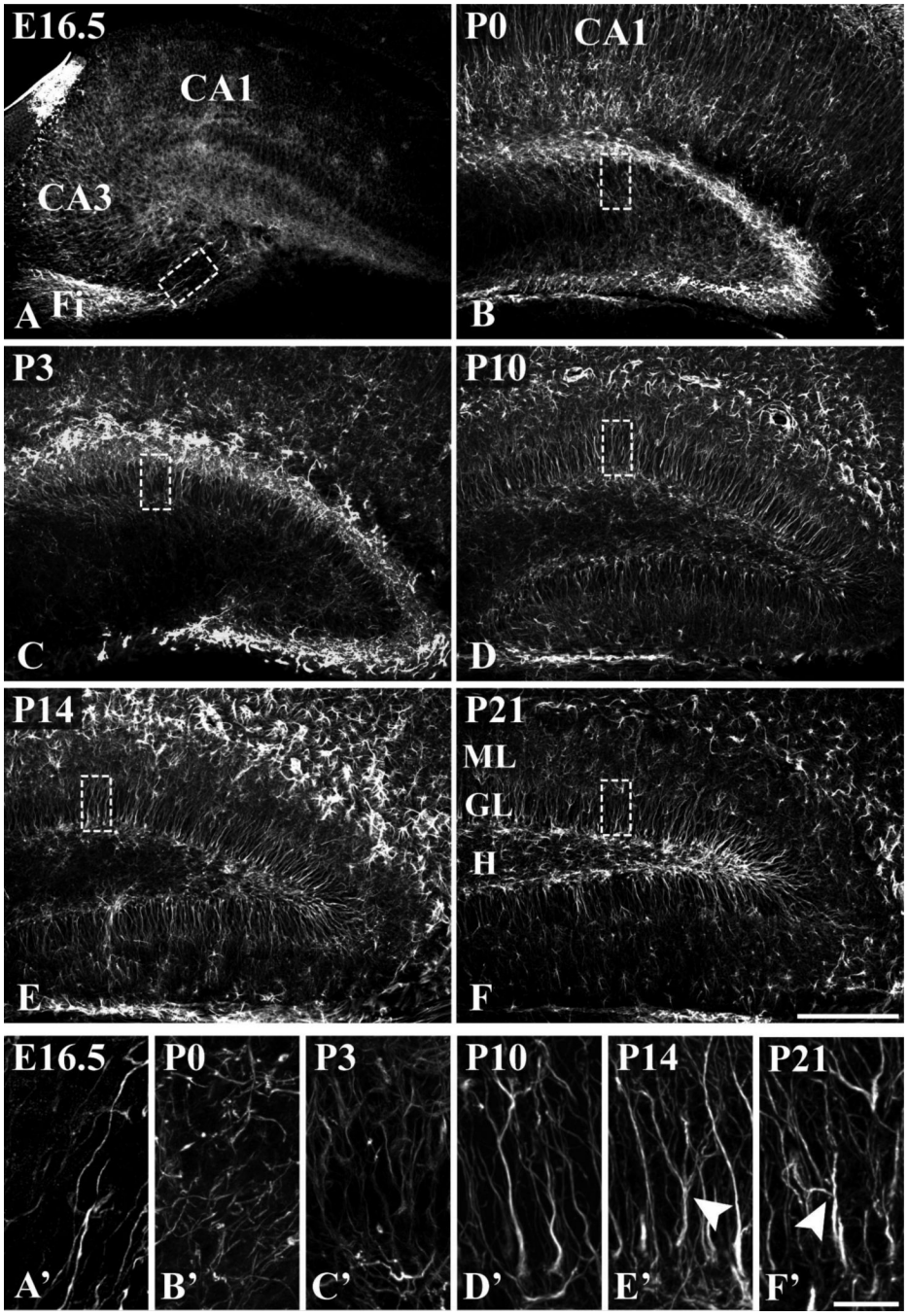

Figure 1. Development of the radial glial scaffold in the murine dentate gyrus

Immunohistochemical visualization of radial glial fibers with a rabbit polyclonal GFAP antibody in coronal hippocampal sections of the indicated developmental stages. The boxed regions are shown at higher magnification in (A'-F'), which are extended focus images from stacks of 10 serial z-sections of 1 μm. **(A,A')** At E16.5, fibers of the primary radial glial scaffold extend from the proliferative zone above the prospective fimbria (Fi) towards the developing suprapyramidal blade of the dentate gyrus. **(B,B')** At P0, GFAP-positive fibers are short and lack a radial arrangement. **(C,C')** Emergence of a secondary radial glial scaffold at P3: radial fibers extend from the hilar region towards the developing molecular layer. **(D-D', E-E')** During the second postnatal week, the secondary radial glial scaffold has fully evolved.

Regularly arranged radial fibers traverse the supra- and infrapyramidal blades of the granular layer. **(F,F')** Secondary scaffold at P21. Note the occurence of branched glial fibers at later stages (arrowheads in E',F'). Astrocytic cells in the outer molecular layer and hilus are also immunolabeled at late stages. Scale bars: 200 μm (A-F), 25 μm (A'-F'). GL, granular layer; H, hilus; ML, molecular layer.

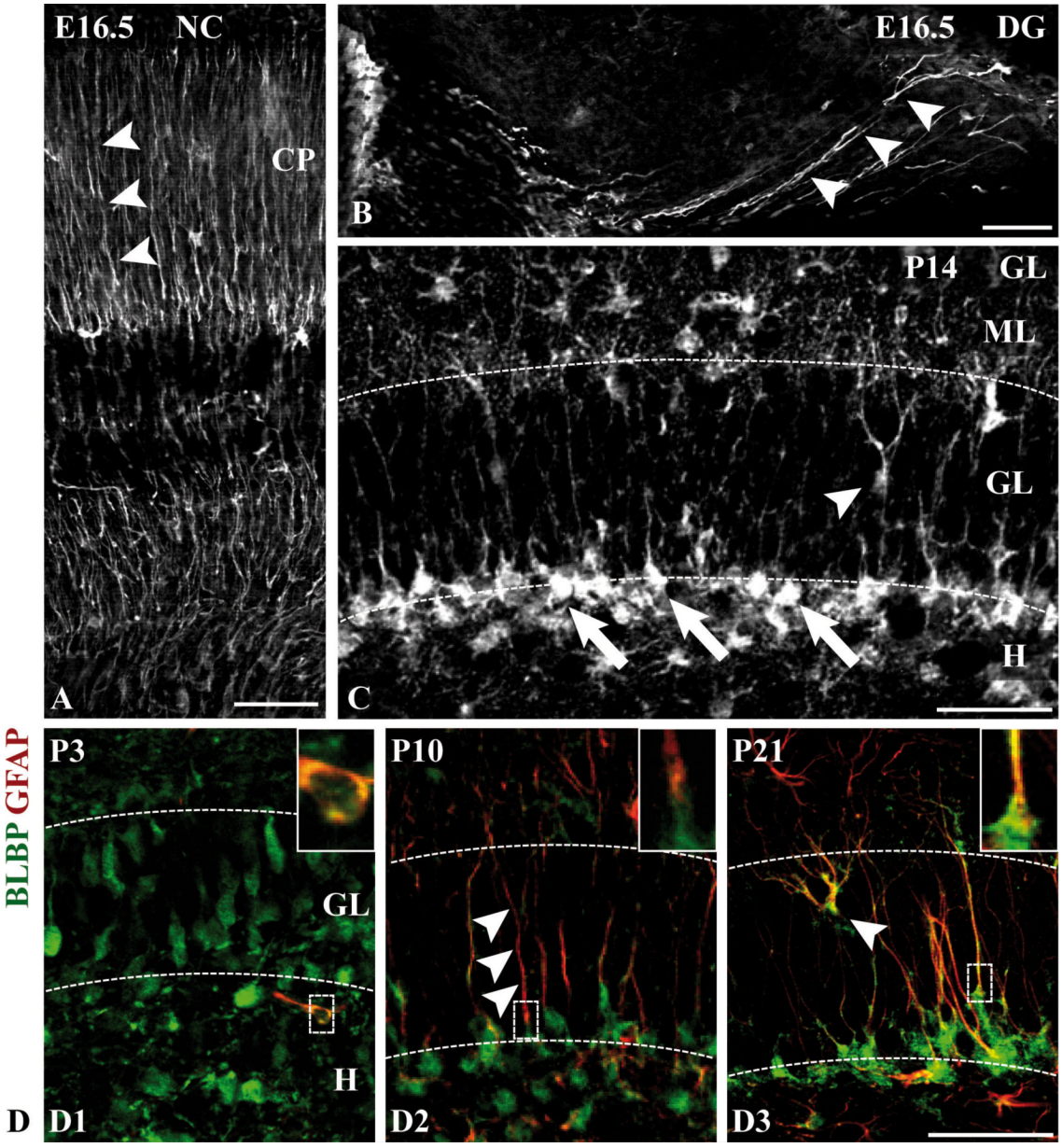

Figure 2. BLBP as radial glial marker in the developing dentate gyrus

(A) Neocortex (NC): BLBP immunolabels radial glial fibers (arrowheads) in the developing cortical plate (CP). **(B)** Dentate gyrus (DG): At E16.5, strong BLBP immunoreactivity is detected in the processes of primordial radial glial cells (arrowheads) in the dentate gyrus (extended focus image from a stack of 10 serial z-sections of 0.55 μm). **(C)** At P14, BLBP immunoreactivity is primarily found in the somata (arrows) of secondary radial glia in the subgranular zone (SGZ). Non-radial BLBP-positive cell bodies are also localized within the GL (arrowhead) and in the ML. **(D)** Hippocampal sections of the developmental stages P3, P10 and P21 were immunostained with an antibody against BLBP (green) and a monoclonal antibody against GFAP (red). The boxed images are magnifications of the cells within the dotted frames and demonstrate colocalization of BLBP and GFAP. The radial processes (arrowheads in D2) are only weakly BLBP-immunoreactive. Note the branched GFAP- and

BLBP-positive cell within the granular layer at P21 (arrowhead, D3). Scale bars: 50 μm. GL, granular layer; H, hilus; ML, molecular layer.

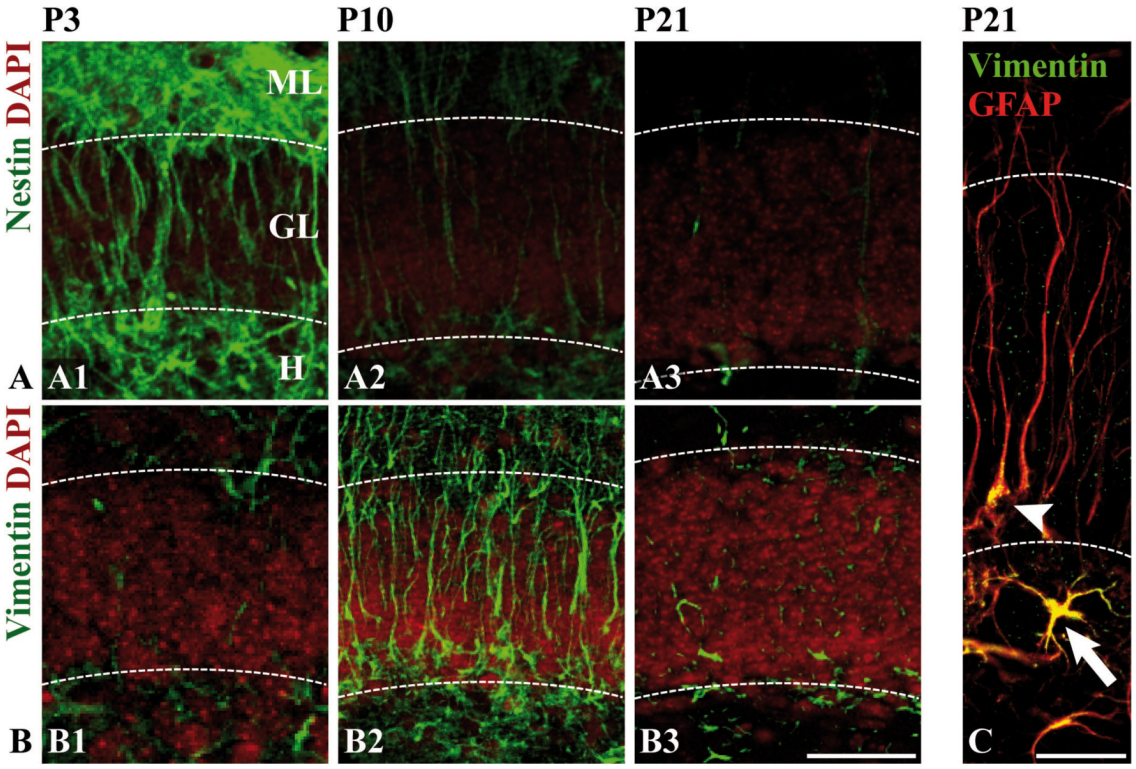

Figure 3. Intermediate filament protein expression in secondary radial glia

Hippocampal sections of the developmental stages P3, P10 and P21 were immunostained with antibodies against nestin **(A1-A3)** or vimentin **(B1-B3)**. Nuclei were counterstained with DAPI (red) to visualize the granule cell layer (GL). Nestin (green) labels secondary radial glial cells at early and intermediate stages (A1-A2), whereas vimentin (green) is a predominant marker at intermediate stages (B2). **(C)** Detection of vimentin in hilar astrocytes (arrow) and radial glia (arrowhead) at P21. Coimmunostaining with the polyclonal GFAP antibody (red) was used to visualize the radial processes. - Scale bars: 50 μm (C: 25 μm).

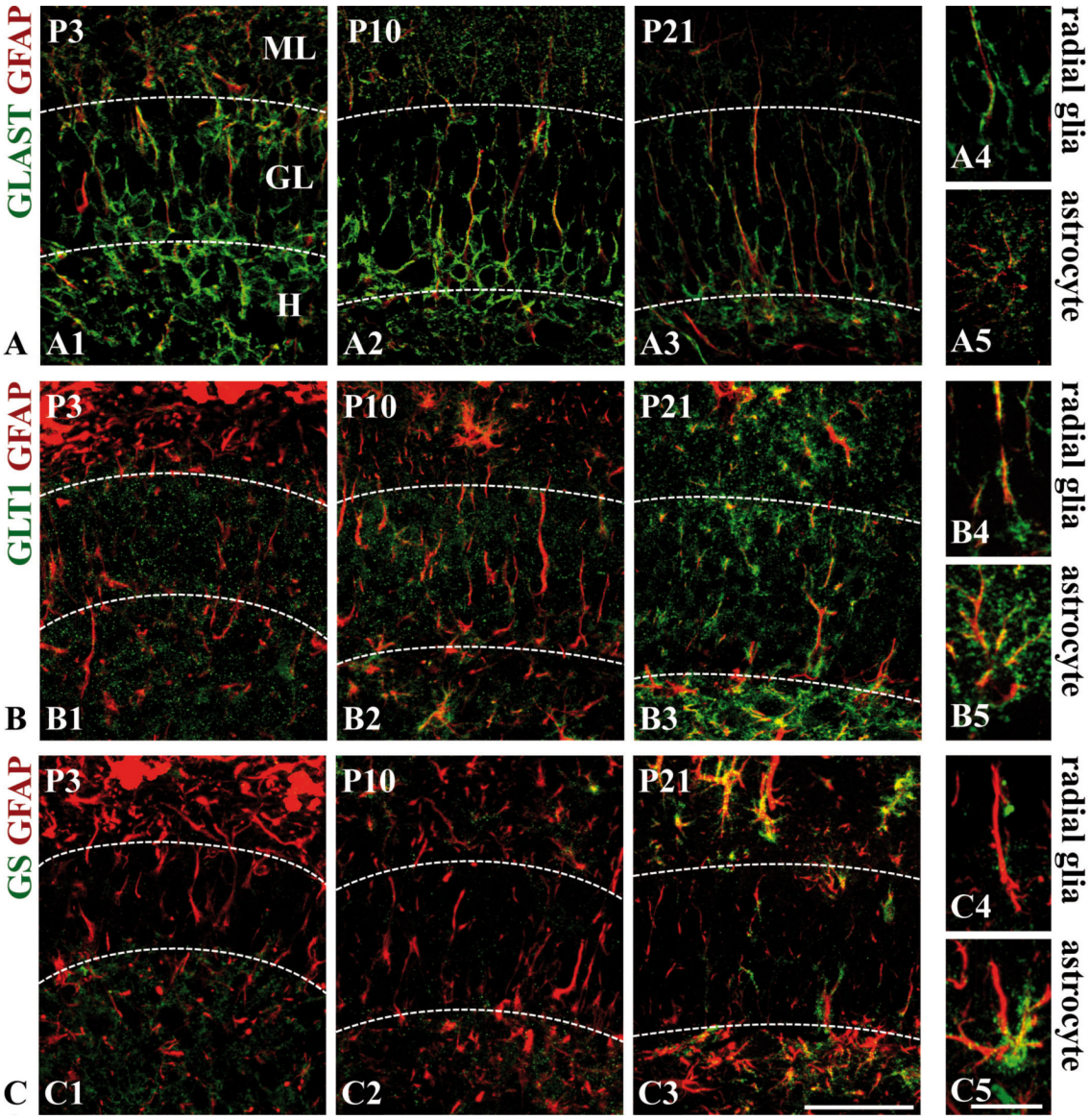

Figure 4. Expression profile of glial markers related to glutamate metabolism in secondary radial glia

Hippocampal sections of the developmental stages P3, P10 and P21 were immunostained with antibodies against GLAST **(A1-A5)**, GLT1 **(B1-B5)**, and glutamine synthetase (GS) **(C1-C5)**. To visualize radial processes, the sections were counterstained with the polyclonal GFAP antibody (red). GLAST immunoreactivity in radial glia was already detected at P3 (A1) and strongest at P10 (A2). (A4) A GLAST-positive radial glial process at P21. Weak GLT1-immunoreactivity of radial glial cells was only seen at late stages (B3-4), whereas no glutamine synthetase expression was detectable in secondary radial glia (C1-C4). GLAST (A5), GLT1 (B5) and glutamine synthetase (C5) expression in astrocytes at P21.

Scale bars: 50 μm (A1-3,B1-3, C1-3), 10 μm (A4-5,B4-5,C4-5). GL, granular layer; H, hilus; ML, molecular layer.

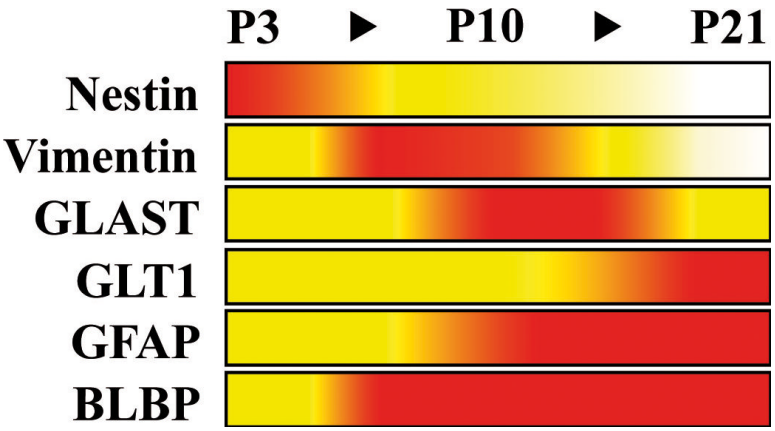

Figure 5. Expression profile of glial marker proteins in secondary radial glia

The relative immunostaining of different glial marker proteins during dentate gyrus development in the secondary radial scaffold is represented by a colour code: White, barely detectable; yellow, moderate immunostaining of many cells or strong labeling of scattered individual cells; red, strong immunoreactivity of many cells. S100-beta and glutamine synthetase are not included; no significant expression of these markers was observed in secondary radial glia.

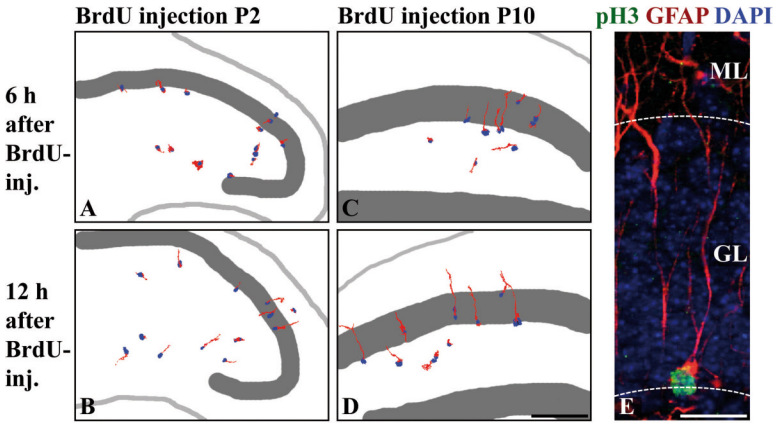

Figure 6. Assembly and proliferative capacity of the secondary radial glial scaffold

(A-D) Proliferating cells in the developing dentate gyrus were birthdated with BrdU (blue) at P2 (A-B) or P10 (C-D) and immunostained for nestin. Processes were reconstructed based on their nestin immunoreactivity (red) using a Photoshop selection tool. (A) 6hr after BrdU-injection, labeled nestin-positive proliferating cells do not yet possess radial processes. (B) 12hr later, the majority of BrdU-labeled cells has outgrown a nestin-positive radial process, indicating that secondary radial glial cells are derived from proliferating cells in the hilus at P2. (C-D) 6 or 12hr after BrdU injection at P10, most of the labeled cells display a nestin-positive radial process, identifying proliferating cells at this stage as belonging to the secondary radial glial scaffold. **(E)** A pH3-positive (green), mitotic secondary radial glial cell at P14, characterized by a long unbranched GFAP-positive process (red) traversing the GL. The soma is localized in the subgranular zone at the border between hilus and GL.

Scale bars: 200 μm (A-D), 25 μm (E). GL, granule cell layer; ML, molecular layer.

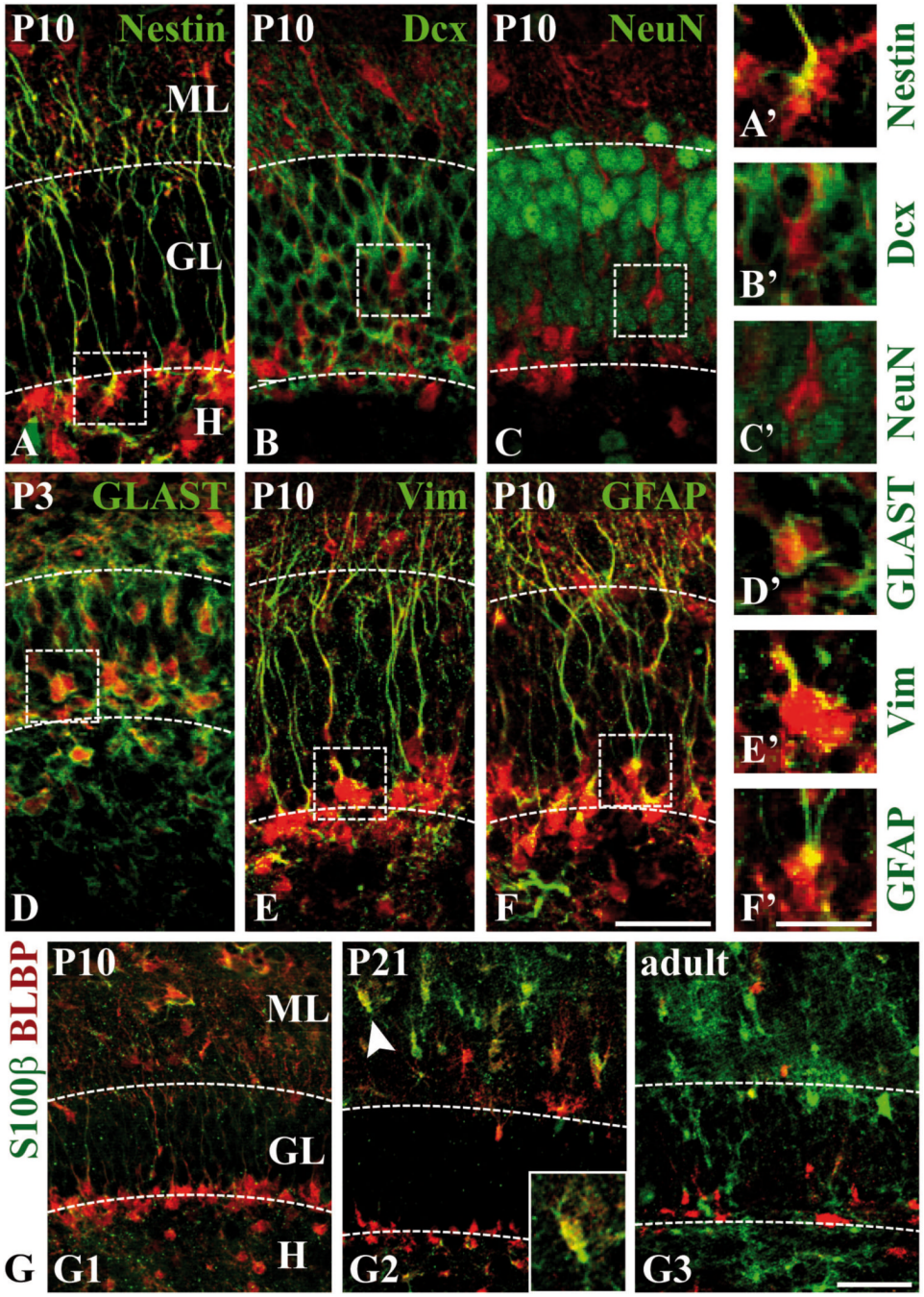

Figure 7. Coexpression of BLBP with astroglial differentiation markers in the developing dentate gyrus

(A-F) Coronal sections of the suprapyramidal granule cell layer at P10 (P3 in D) were coimmunostained with antibodies against BLBP (red) and the indicated marker (green). The boxed regions are shown at higher magnification in (A'-F'). (A) A strong colocalization of BLBP and the precursor cell marker nestin is detected in radial glial cells in the subgranular zone. (B-C) No colocalization of BLBP with the neuronal markers doublecortin (Dcx) (B) or NeuN (C) can be observed. (D) Double-labeling of BLBP and GLAST is most prominent at P3. (E-F) Colocalization of BLBP with vimentin (Vim) and GFAP (immunolabeled with the mouse monoclonal antibody) in the secondary radial glial scaffold peaks in the second postnatal

week. **(G1-G3)** Coimmunostaining of BLBP (red) and S100-beta (green) at P10, P21 and in adult mice. Occasional colocalization of both markers in astroglial cells of the inner ML is observed at P21 (G2). The inset shows one of the double-labeled cells (arrowhead) at higher magnification. Coexpression is neither seen at P10, where almost no S100-beta can be observed (G1), nor in adult mice, where BLBP-positive cells in the ML are rarely detected (G3). Note the increase in S100-beta expression over time.
Scale bars: 50 μm (A-F, G1-G3), 25 μm (A'-F', G2',G2''). GL, granule cell layer; ML, molecular layer.

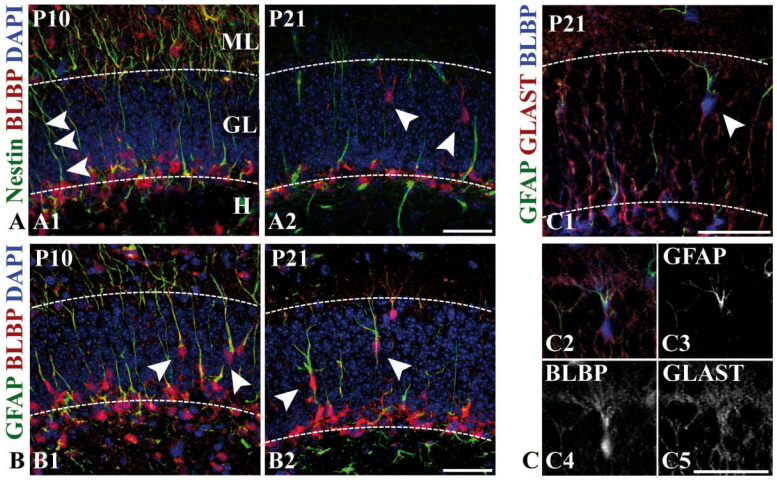

Figure 8. Immunohistochemical characterization of transforming secondary radial glia

(A1-A2) At P10 (A1), BLBP (red) and nestin (green) are colocalized in secondary radial glial cells, which extend unbranched radial processes through the granule cell layer. At P21 (A2), BLBP-positive cells whose somata are located within the granular layer extend branched processes, which are negative for nestin (arrowheads). Nuclei were counterstained with DAPI. **(B1-B2)**, Colocalization of BLBP (red) and GFAP (green, monoclonal antibody) at P10 and P21. At P10 (B1), somata of double-immunolabeled radial glial cells with unbranched processes are localized within the granule cell layer (arrowheads). At P21 (B2), BLBP-positive cells whose somata are located within the granular layer extend branched GFAP-immunoreactive processes (arrowheads). Nuclei were counterstained with DAPI. (**C1-C5)** Triple-immunostaining of a hippocampal section at P21 with antibodies against BLBP (blue), GLAST (red) and GFAP (green, monoclonal antibody). (C2) Single-channel views of the triple-labeled cell (arrowhead in C1) are shown in C3-C5. Note the membranous punctuate GLAST immunoractivity (C5). - Scale bars: 50 μm.

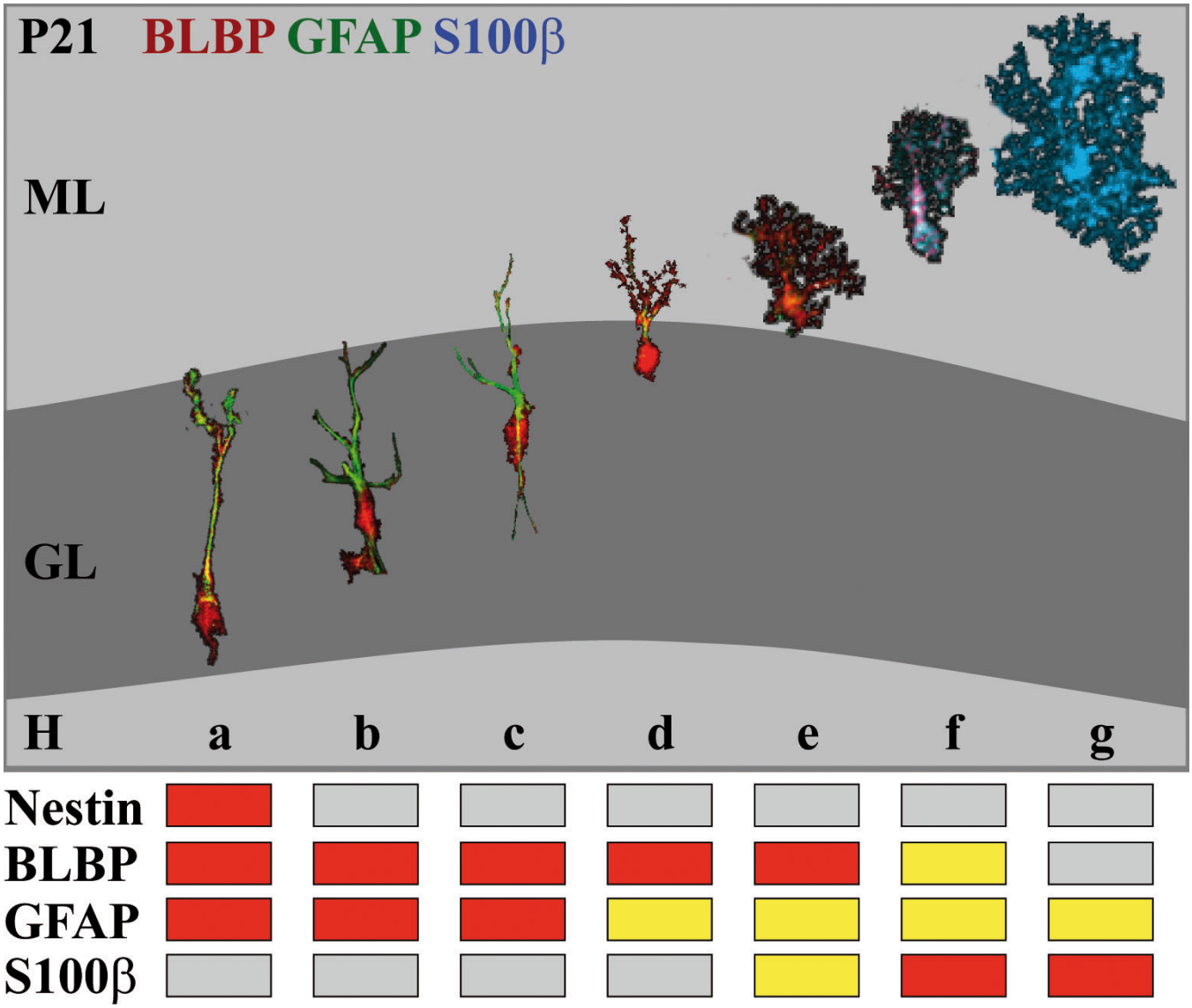

Figure 9. A model of radial glial migration and astrocytic transformation in the developing dentate gyrus

(a) The somata of secondary radial glial cells in the developing dentate gyrus are located in the subgranular zone and extend long radial processes that traverse the granular layer (GL). At this stage secondary radial glia with progenitor cell properties express nestin, BLBP (red) and GFAP (green). Astroglial differentiation is characterized by downregulation of nestin expression (b) and morphological changes: the BLBP-positive soma translocates from the subgranular zone into the granule cell layer, while the GFAP-positive process starts to ramify within the granular layer. Increasing branching of the processes occurs while the cells translocate through the GL towards the molecular layer (ML) (b-d). Immature astrocytes at the border to and within the ML start to express S100-beta and gradually lose BLBP expression (d-f). Mature astrocytes in the molecular layer are characterized by the expression of S100-beta and in some cases of GFAP (g). – All of the displayed stages of radial glial transformation were taken from sections of 21 day-old mice using a Photoshop selection tool. The grading of the immunstaining was colour-coded as described in Figure 5.

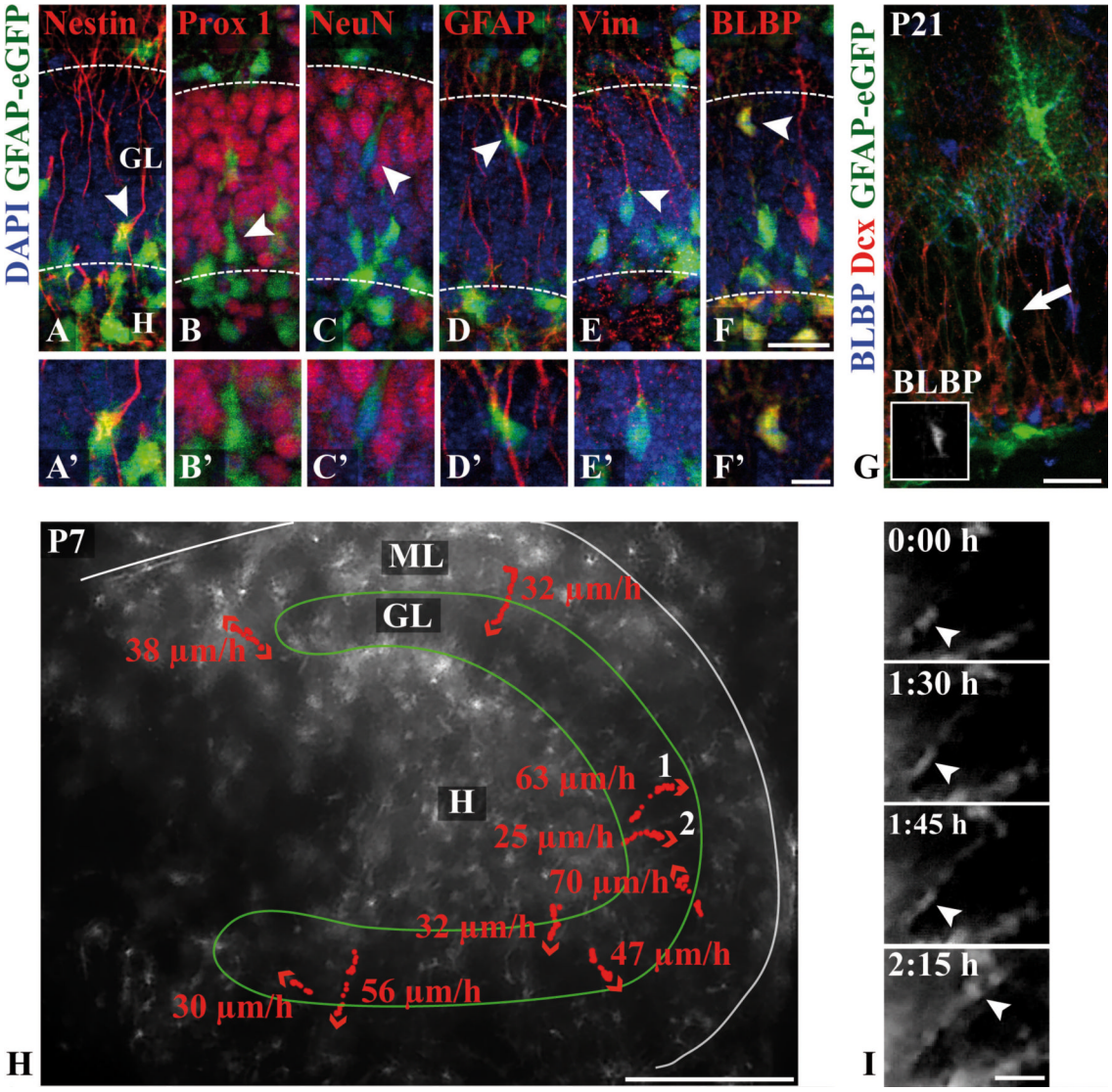

Figure 10. In vivo imaging of astroglial migration in the developing murine dentate gyrus

(A-F) Immunohistochemical characterization of GFP-fluorescent cells in the dentate gyrus of P7 hGFAP-eGFP transgenic mice. Coronal sections were immunostained with antibodies against the indicated markers (red) and counterstained with DAPI (blue). Colocalization of GFP fluorescence (green) with nestin (A) and astroglial (D-F) but not with neuronal markers (B-C) is observed (arrowheads). Magnifications of the marked cells are shown in (A'-F'). **(G)** Colocalization of BLBP (blue) and GFP fluorescence in a translocating glial cell (arrow) whose soma is located in the middle of the granular layer (inset in G to show single BLBP staining). No colocalization of GFP fluorescence and Dcx (red) is observed. **(H)** Fluorescent live microscopy of a hippocampal slice culture prepared from a P7 hGFAP-eGFP transgenic mouse. The positions of different cells were monitored every 15 min and marked by red dots. The arrowheads indicate the direction of migrating cells. The maximal cell speed (µm/hr) of the highlighted cells are indicated. A total of 19 cells from two different preparations were analyzed. **(I)** Fluorescent time-lapse images of cell 1 (arrowhead: soma).

Scale bars: 25 µm (A-F,I), 10 µm (A'-F'), 50 µm (G), 200 µm (H). Dcx, doublecortin; GL, granular layer; H, hilus; ML, molecular layer; Vim, vimentin.

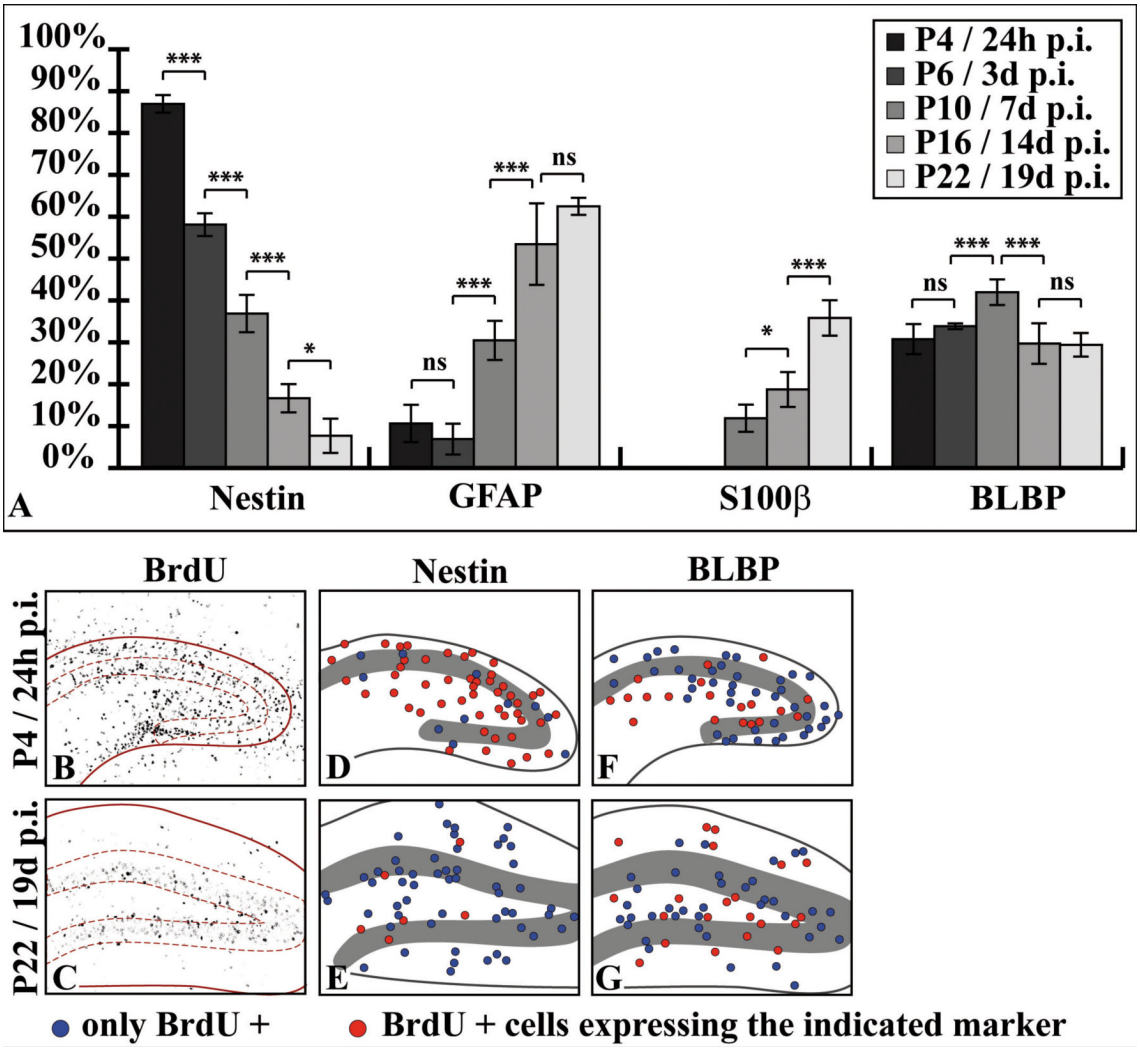

Figure 11. Immunohistochemical profiling of P3-birthdated progenitor cells at various stages of dentate gyrus development

(A) The diagram shows the percentage (mean ±SD) of BrdU-labeled cells expressing nestin, GFAP, S100-beta or BLBP at the indicated time points after BrdU injection at P3 (n=180 cells). Differentiating cells quickly downregulate nestin, while GFAP and S100-beta are upregulated. BLBP expression did not change much during the period investigated. **(B-C)** Proliferating cells in the dentate gyrus were BrdU-labeled at P3 and tracked 24hr (P4) and 19 days (P22) post injection (p.i.). (B) 24hr p.i., BrdU-labeled cells are distributed over the entire area of the developing hippocampus. (C) At P22, the cells that were labeled at P3 are primarily found in the subgranular zone and in the granular layer. **(D-G)** To determine the redistribution of labeled cells during development, 20 BrdU-positive cells in the hilus, granular and molecular layer were arbitrarily chosen and tested for expression of nestin (D-E) or BLBP (F-G), respectively. Blue circles indicate BrdU-only positive cells, red circles represent BrdU-positive cells that express the respective marker. Most of the BrdU-labeled cells are nestin-positive at P4 (D), whereas double-labeled cells at P22 are rare and mostly confined to the subgranular zone (E). BLBP-positive BrdU-positive cells are scattered over the dentate area at P4 (F) and redistribute to the hilus, molecular layer and subgranular zone at P22 (G).

Table 1

List of primary and secondary antibodies.

Antigen	Species	Dilution	Company	Order Number
BLBP	rabbit IgG	1:500	Millipore	AB9558
BrdU	rat IgG	1:1000	Abcam	6326-250
Doublecortin	goat IgG	1:1000	Santa Cruz	sc-8066
GFAP	rabbit IgG	1:500	Dako Cytomation	Z0334
GFAP	mouse IgG	1:500	Sigma-Aldrich	G3893
GLAST	guinea pig IgG	1:500	Millipore	AB1782
GLT1	guinea pig IgG	1:4000	Millipore	AB1783
Glutamine synthetase	mouse IgG	1:500	Millipore	MAB 302
Nestin (Rat401)	mouse IgG	1:30	DSHB	Rat401
NeuN	mouse IgG	1:1000	Millipore	MAB377
NG2	rabbit IgG	1:3000	Millipore	AB5320
PGP9.5	rabbit IgG	1:2000	Neuromics	RA12103-30
p-histone H3 (pH3)	rabbit IgG	1:500	Millipore	06-570
Prox1	rabbit IgG	1:500	Millipore	AB5475
S100-beta	mouse IgG	1:500	Sigma	S2532
Vimentin (40EC)	mouse IgM	1:20	DSHB	40EC

Antigen	Label	Dilution	Company	Order Number
mouse IgG	AF555	1:1000	Invitrogen	A31570
mouse IgG	AF488	1:1000	Invitrogen	A21202
mouse IgM	AF555	1:1000	Invitrogen	A21426
mouse IgM	AF488	1:1000	Invitrogen	A21042
rabbit IgG	AF488	1:1000	Invitrogen	A21206
goat IgG	AF555	1:1000	Invitrogen	A21432
guinea pig IgG	AF568	1:1000	Invitrogen	A11075
rat IgG	Biotin	1:100	Vector	BA-4001

Abbreviations: AF, Alexa Fluor; DSHB, Developmental Studies Hybridoma Bank.